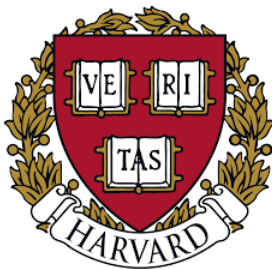


# POLITECNICO DI TORINO

Master's Degree in Biomedical Engineering

## Gait Analysis for X-linked Dystonia Parkinsonism

Disease Assessment and Severity Estimation Using  
Sensing Technology and Machine Learning



**Supervisors**

**Prof. Danilo Demarchi**

**Prof. Paolo Bonato**

**Dr. Giulia Corniani**

**Candidate**

**Stefania Sanseverino**

**A.A. 2023-2024**



# Table of Contents

<b>Acknowledgements</b>	5
<b>Abstract</b>	8
<b>1 Introduction</b>	10
1.1 X-Linked Dystonia Parkinsonism (XDP)	10
1.1.1 Parkinson’s disease	11
1.1.2 Dystonia disease	12
1.2 XDP phenotype and consequences	15
1.3 Aim of the project	17
<b>2 State of the art</b>	19
<b>3 Materials and methods</b>	22
3.1 Materials and experimental set up	22
3.1.1 IMU sensors	23
3.1.2 Xsens	27
3.2 Data collection	29
3.2.1 Subjects	29
3.2.2 Tasks and UPDRS scale	32
3.3 Methods	36
3.3.1 Pre-processing	38
3.3.2 Gait analysis	40
3.3.3 Feature extraction and dataset construction	43
3.3.4 Feature selection	46
3.3.5 Feature projection	53
3.3.6 Classification	54
<b>4 Results and discussion</b>	56
4.1 Gait task	56
4.1.1 Feature projection	56
4.1.2 Classification	57
4.1.3 Feature assessment	58
4.2 Freezing of gait task	61
4.2.1 Feature projection	61
4.2.2 Classification	62
4.2.3 Feature assessment	63

4.3	Postural instability task . . . . .	64
4.3.1	Feature projection . . . . .	65
4.3.2	Classification . . . . .	65
<b>5</b>	<b>Conclusion</b>	<b>67</b>
	<b>List of Tables</b>	<b>69</b>
	<b>List of Figures</b>	<b>70</b>
	<b>Bibliography</b>	<b>72</b>



# Acknowledgements

I would like to express my heartfelt gratitude to Prof. Danilo Demarchi from Politecnico di Torino for paving the way for this invaluable experience at Spaulding Rehabilitation Hospital. I also wish to extend my sincere thanks to Professor Paolo Bonato and Dr. Giulia Corniani for their unwavering supervision and guidance throughout my time in Boston.

*Ai miei genitori*, questo traguardo è per voi. Grazie per aver reso tutto possibile fin qui, per aver accettato ogni mia richiesta seppur molto grande, grazie per non avermi fatto pesare una sola delle mie scelte e per aver sempre creduto in quel che sono e faccio. Non dimenticherò mai il grande sacrificio che avete fatto ogni giorno affinché arrivassi fin qui. Grazie.

*A Maira ed Alessio*, grazie per essere sempre così premurosi, per aver fatto un viaggio oltreoceano per incontrarmi e per avermi fatto sentire sempre il vostro affetto, nonostante le mie chiamate sporadiche.

Alle mie migliori amiche, *Irenea ed Alessia*, il nostro legame l'ho sentito anche dall'altra parte del mondo. Un grazie infinito per essere sempre al mio fianco, per avermi sempre supportata ed ascoltata, soprattutto in questi mesi di turbolenza per me. Non è scontato avervi, vi voglio un bene dell'anima.

*A tutti i miei amici divisi tra nord e sud.*

Un grazie a *Giorgia*, perfetta amica e mia compagna in quest'avventura al PoliTO in cui abbiamo condiviso risate, notti in bianco, fobia per gli insetti e disavventure universitarie. La bellezza di essere l'una la spalla dell'altra in questi anni non la dimenticherò mai, anche a distanza.

Un grazie *alla mia famiglia torinese*, in particolare a *Marco, Tiziano, Monica e Francesco* per aver scelto di trasformare l'ultimo Natale in un viaggio magico con me, dall'altra parte del mondo. Grazie per avermi portato 'casa' in America, è stato indimenticabile.

Grazie anche a *Chiara*, in breve tempo ci siamo subito trovate affini. Tra chiacchierate e colazioni chic, non dimenticherò il tuo profondo

supporto soprattutto nell'ultimo periodo a Torino.

Un grazie a casa 2 *To.sta* e ai suoi inquilini, che hanno consentito lo sviluppo di un rapporto speciale tra convivi, partite, panzerotti, vino e tante risate. Grazie a *Moni*, sempre pronta ad una chiamata per ascoltare e dare consigli. E grazie anche a *Franco e Titti*, tutte le avventure a Torino e le 'gite' fuori-porta con voi le porterò sempre nel cuore. Se Torino è diventata casa è soprattutto grazie a voi.

Un ringraziamento particolare a *Brontolo*, abbiamo condiviso quasi l'intero percorso universitario tra triennale e magistrale, diviso tra nord/sud e tantissimi cambiamenti che non hanno fatto cambiare il nostro rapporto nemmeno a distanza.

A *Matti*, è stata un'incredibile sorpresa incontrarsi nell'ultimo periodo lì. In così poco tempo abbiamo un bagaglio ricco di ricordi assieme sparsi in tutta l'America, tra deserti e boschi. Il viaggio continua.

A tutto il *MAL*, che consente un perfetto incontro di mondi e che mi ha dato la possibilità di incontrare persone magnifiche da ogni parte del globo. È stato una splendida avventura.



# Abstract

X-linked dystonia parkinsonism (XDP) is a rare movement disorder seen primarily in individuals from Panay Island, Philippines, marked by adult-onset dystonia that gradually progresses and often transitions into parkinsonism. The aim of this project is to assess the severity of XDP symptoms across four specific conditions (gait, freezing of gait, postural instability, and posture) by extracting relevant features from signals acquired through Inertial Measurement Unit (IMU) wearable sensors. The same approach was used to achieve this goal for each of these tasks. The dataset comprises baseline and follow-up data. The baseline includes 5 controls and 32 XDP subjects. Follow-up data were collected from 13 XDP subjects at 6 months and 7 XDP subjects at 12 months after the baseline. Disease severity was assessed with the Unified Parkinson's Disease Rating Scale Part 3 (MDS-UPDRS). Data collections were performed using 17 9-axis IMUs, and suitable data features were derived to estimate clinical scores using machine learning (ML).

A certain number of features were selected using Recursive Feature Elimination (RFE), and a feature projection for each lower limb task was performed to inspect the clustering between patients before classification. An ML supervised algorithm was then developed to predict the scores using the Random Forest algorithm with the Leave-One-Out Cross-Validation method. Gait spatio-temporal parameters and frequency-specific features play a crucial role, as the results demonstrate a high degree of clustering between different stages of the disease. However, there is a margin for improvement that could be achieved with a more balanced dataset.

This study assessed the feasibility of using wearable sensors to evaluate gait patterns in XDP patients and derived reliable clinical score estimates. The results suggest that wearable technology, combined with advanced feature selection and machine learning algorithms, can be a powerful tool in monitoring and evaluating the progression of movement disorders such as XDP. Further research with larger and more balanced datasets could enhance the accuracy and reliability of these methods, providing valuable insights for clinical assessments.



# 1. Introduction

The central aim of this project is to analyze the movements of patients affected by the rare neurogenetic movement disorder known as X-linked Dystonia-Parkinsonism (XDP). The study's primary objectives are twofold: first, to detect the presence of characteristic dystonic movements, and second, to implement a scoring system based on the Unified Parkinson's Disease Rating Scale (UPDRS). To achieve the study's aims, wearable sensor technology was employed, combined with deep feature analysis and advanced machine learning algorithms. This integrated approach allows for the identification of disease-specific variables, quantification of the disorder, and monitoring of its progression in patients.

To fully grasp the context and significance of the study, it is essential to highlight the key elements that will be elaborated upon in this research.

## 1.1 X-Linked Dystonia Parkinsonism (XDP)

X-Linked Dystonia Parkinsonism (XDP) is an uncommon inherited neurogenetic movement disorder. It shows a notable gender difference, primarily affecting Filipino men more than women. On Panay Island, where XDP is prevalent, the disease occurs at a rate of about 5.74 cases per 100,000 people. The province of Capiz, in particular, has the highest prevalence rate, with 18.9 cases per 100,000 individuals [1]. The distinct demographic pattern of XDP highlights the necessity of understanding both genetic and environmental factors that contribute to the disorder in this population. Further investigation into the underlying causes and potential treatments can offer valuable insights into the interaction between genetics and environmental factors in movement disorders, thereby advancing clinical knowledge and patient care. XDP is a neurodegenerative condition linked to a mutation on the X chromosome, caused by the insertion of an antisense SINE-VNTR-Alu (SVA)-type retrotransposon within a TAF1 intron. This insertion is accompanied by six additional noncoding sequence changes in TAF1, the gene encoding TATA-binding protein-associated factor-1. These sequence changes appear to be inherited together, forming an identical haplotype seen in all reported cases[2]. In essence, XDP results from

the combination of two well-known neurological disorders, Dystonia and Parkinson's disease. This unique combination highlights the complex interplay of pathophysiological mechanisms that contribute to this specific neurodegenerative condition.

### 1.1.1 Parkinson's disease

Parkinson's disease is recognized as the second most common neurodegenerative disorder worldwide, following Alzheimer's disease. The prevalence of Parkinson's disease is higher in Europe, North America, and South America, whereas African, Asian, and Arabic countries have lower prevalence rates.[3] Despite its growing impact, diagnosing Parkinson's disease remains complex and challenging. Understanding the nuances of the earliest stages of the disease is a critical, unmet need, emphasizing the importance of improving early detection methods and interventions. Such advancements could enhance our knowledge and management of this intricate neurodegenerative condition. Parkinson's disease is caused by the gradual loss of dopamine-producing neurons in the brain's substantia nigra and is marked by various motor and non-motor symptoms.[4]

#### **Motor and non-motor symptoms[5]**

Motor symptoms refer to the physical and movement-related signs of the condition, including:

- Muscle rigidity involves stiffness in the limbs, limiting the range of motion. Although the speed of finger tapping might remain normal, the amplitude of movement is significantly reduced, particularly affecting hand movements.
- Tremors are involuntary shakes or trembles, often starting in one limb. Unlike the typical tremor seen in essential tremor, the tremor associated with Parkinson's disease has a slower frequency and occurs when the limb is at rest.
- Postural instability is difficulty in maintaining balance and coordination. Patients may experience a phenomenon called festination, where the trunk moves ahead of the feet. To regain balance, individuals may take small, rapid steps resembling a running motion.

- Bradykinesia refers to the slowness of movement, making simple tasks take longer. It involves a reduction in spontaneous movement, leading to 'masked facies' or hypomimia, which is characterized by reduced movement of facial muscles, resulting in a less expressive facial appearance.

Conversely, non-motor symptoms encompass a wide range of manifestations that go beyond the usual movement-related impairments linked to the condition. These symptoms can greatly affect the overall well-being and quality of life for individuals with Parkinson's. Some examples of these symptoms include:

- Cognitive changes: Parkinson's disease can lead to cognitive decline and dementia, especially in the later stages.
- Autonomic dysfunction: problems with regulating automatic bodily functions, resulting in issues like changes in blood pressure, constipation, and abnormal sweating.
- Mood disorders: depression and anxiety are frequently experienced by people with Parkinson's.
- Sleep disturbances: many individuals report difficulties with falling asleep or staying asleep.
- Anosmia: loss of the sense of smell can occur many years before other symptoms appear.

### 1.1.2 Dystonia disease

Dystonia is the third most prevalent movement disorder, following Parkinson's disease and essential tremor. This ranking underscores its importance within the realm of movement disorders and highlights its clinical significance in neurological conditions. Given its prevalence and impact on motor functions and quality of life, further exploration and understanding of dystonia are essential, making it a critical area for scientific research and therapeutic development [6]. Dystonia involves

sustained or intermittent muscle contractions that cause abnormal and often repetitive movements or postures. These movements are characterized by their patterned, twisting nature and sometimes tremulous quality, emphasizing the complex motor disturbances associated with the condition. Dystonia is also unique in that it can be influenced by voluntary actions, creating an interplay between voluntary and involuntary muscle activity. Overflow muscle activation further illustrates the multifaceted nature of dystonia, highlighting the intricate neurophysiological mechanisms at play [balint2018dystonia, 7]. To thoroughly characterize dystonia, four essential descriptors are used: age at onset, body distribution, temporal pattern, and associated features [6, 7].

### **Age at onset**

The age at onset is a crucial factor in the clinical context of dystonia, influencing both diagnosis and prognosis. It helps in identifying specific types of dystonia and guides the customization of treatments to meet the individual needs of patients. This temporal aspect is a valuable tool for healthcare providers, allowing them to offer more accurate and personalized advice, as well as to predict and manage the progression of the disease effectively.

### **Body distribution**

Dystonia, affecting various body regions, highlights the diverse nature of this neurological disorder. Understanding the specific forms based on the location and type of involvement is essential for a comprehensive grasp of the condition. This classification aids in accurate diagnosis and customized treatments, acknowledging that dystonia's presentation can vary greatly depending on the affected regions and patterns of involvement. Specifically, dystonia can be categorized as follows:

- Focal dystonia localized to a specific area, such as the neck, hand, or face. Common types include Cervical Dystonia, Blepharospasm, Oromandibular Dystonia, and Laryngeal Dystonia.
- Segmental dystonia involves two or more adjacent body regions. Examples include cranial dystonia, characterized by conditions such as blepharospasm combined with lower facial and jaw or tongue involvement, and bibrachial dystonia.

- Multifocal dystonia affects two or more body regions, either contiguous or noncontiguous.
- Generalized dystonia involves the trunk along with at least two additional body sites. This category differentiates between forms where the legs are affected and those without leg involvement.
- Hemidystonia affects multiple body regions confined to one side of the body.

### **Temporal pattern**

The dynamic nature of symptoms and their varying severity over time highlight the diversity within dystonia, allowing for a nuanced classification into static and progressive forms. This temporal variability impacts clinical presentation and significantly influences prognosis and treatment strategies. Recognizing this dynamic aspect is crucial for healthcare providers to tailor interventions, monitor disease progression, and offer informed prognostic information to patients with dystonia. Additionally, the evolving nature of symptoms underscores the need for longitudinal studies to thoroughly understand the underlying mechanisms and factors contributing to the fluctuating course of dystonic conditions. The temporal fluctuations in dystonia's presentation can be categorized into four distinct types:

- Persistent: dystonia that remains consistent throughout the day with relatively uniform intensity.
- Paroxysmal: dystonic episodes that are transient and typically triggered by specific stimuli, with the patient returning to their previous neurological state afterward.
- Diurnal fluctuations: dystonia's characteristics, intensity, and occurrence exhibit noticeable variations according to a clear circadian rhythm.
- Action-specific: dystonic movements that occur only during the performance of a highly specific task.

### Associated features

Dystonia can appear as a sole observable phenotype, demonstrating its ability to manifest independently. However, it can also coexist with other movement disorders, indicating the complex interplay of different neurological conditions. This variability highlights the diverse clinical manifestations of dystonia and underscores the importance of comprehensive assessments to determine whether it occurs alone or in conjunction with other movement disorders. Based on this aspect, distinctions can be made among:

- Isolated Dystonia form is characterized by dystonia as the only motor feature, with tremor being the only exception.
- Combined Dystonia form includes the presence of additional movement disorders, such as parkinsonism, myoclonus, or dyskinesia, alongside dystonia.
- Complex Dystonia involves dystonia along with other neurological or systemic manifestations. In many of these syndromes, dystonia may be an intermittent feature or not the primary manifestation of the disease.

## 1.2 XDP phenotype and consequences

X-linked Dystonia-Parkinsonism (XDP) is a rare neurodegenerative condition mainly affecting individuals of Filipino descent, particularly those from Panay Island. According to the current XDP study registry, there are 505 documented cases from 253 different families. The disorder exhibits a significant male bias, with a male-to-female ratio of 100:1, which is a key characteristic of its pathology. This pronounced gender difference prompts further exploration into the genetic factors or mechanisms underlying the higher incidence in males. In all documented female cases, the women have affected relatives, suggesting a likely connection to carrier mothers. This familial pattern supports the X-linked inheritance of XDP, where carrier mothers pass on the genetic mutation, resulting in the disorder in their children. XDP typically begins to manifest between the ages of 39 and 40, with onset ranging from 12 to 64 years. The disorder usually lasts about 16 years,

highlighting its chronic nature. On average, individuals with XDP die around the age of 55.6 years, providing insights into the disease's duration and its impact on life expectancy. Initially, XDP presents with focal dystonia that tends to generalize over time. The common clinical manifestations of dystonia, organized by region and roughly in descending order of frequency, include:

- Lower extremities: big toe dorsiflexion ("striatal toe"), foot extension/flexion/inversion, toe fanning, and knee extension/flexion.
- Craniofacial region: jaw opening, closing, and deviation; tongue protrusion, rolling, and retraction; blepharospasm; facial twitching; mouth pursing; snout-like movements of lips; and adductor laryngeal dysphonia.
- Neck and shoulder regions: rotational (torticollis), laterocollis, retrocollis, anterocollis (or combinations thereof), with or without shoulder elevation.
- Upper extremities: wrist extension/flexion, writer's cramp involving fingers, and elbow extension/flexion.
- Truncal region: spinal flexion/extension/lateral deviation (or combinations thereof) and flexion at the pelvis or camptocormia.

This categorization offers a structured overview of the diverse clinical manifestations of dystonia across different anatomical regions. As dystonia symptoms lessen, Parkinsonian features begin to appear. In some patients, these Parkinsonian symptoms can closely resemble those of idiopathic Parkinson's disease (PD), including resting tremor, rigidity, and bradykinesia.

About the effects, the XDP disease leads to a range of motor and non-motor impairments that profoundly affect those with the condition. The repercussions of X-linked Dystonia-Parkinsonism extend beyond physical symptoms, impacting various facets of overall well-being. This includes:

- Psychosocial challenges: individuals often face emotional distress, anxiety, and depression due to the progressive nature of XDP and

its motor impairments, significantly affecting mental health. Many individuals may initially deny these emotional struggles, which can lead to harmful behaviors such as substance abuse, including alcohol and drug use.

- Social isolation: motor symptoms, particularly those affecting facial expressions and speech, can lead to withdrawal from social interactions. This can result in social isolation, loneliness, and reduced social engagement due to communication difficulties.
- Cognitive and emotional impact: cognitive impairments, such as difficulties with executive functions, can affect everyday decision-making and problem-solving abilities. Emotionally, individuals may experience frustration, grief, and a sense of loss as they deal with the ongoing challenges of the condition.
- Financial strain: the financial burden of managing a chronic illness like XDP can be significant. Medical expenses, the cost of assistive devices, caregiving costs, and potential loss of income can create substantial stress for both the affected individuals and their families.

## 1.3 Aim of the project

This project aims to analyze the motion in XDP patients, an area that remains largely unexplored in current literature. Parkinsonism and dystonia are closely related due to the significant overlap in their symptoms. While existing research delves into motion analysis concerning Parkinson's disease and dystonia, it does not specifically address X-linked dystonia. The convergence of these two distinct movement disorders presents a challenge for clinicians, complicating the accurate scoring and assessment of the pathology. The subjective nature of clinical evaluations further exacerbates this challenge, introducing variability in diagnostic judgments. Additionally, the late recognition of XDP symptoms, especially in the advanced stages, adds another layer of complexity. This delay in identification can impede timely intervention and the initiation of appropriate treatment strategies. Therefore, addressing the subjective elements in the diagnostic process and promoting early recognition of XDP are crucial for improving clinical outcomes and enhancing patient care in this unique neurodegenerative disorder.

Furthermore, the challenge of subjectivity in clinical evaluation is particularly pronounced in this case. Diagnosing the disease is complex, and only highly specialized and experienced clinicians can accurately identify symptoms at the onset. However, given the phenotype of XDP, individuals are often located in remote areas and villages with limited access to specialized medical expertise. Developing an automatic assessment tool can offer a solution, providing objective diagnostic tools that are universally accessible.

## 2. State of the art

Dystonia, a movement disorder characterized by involuntary muscle contractions leading to abnormal postures and repetitive movements, requires a multifaceted approach for assessment. Traditionally, clinical scales such as the Burke-Fahn-Marsden Dystonia Rating Scale (BFMDRS) and the Global Dystonia Rating Scale (GDS) have been used to provide qualitative measures based on observed movement abnormalities [7]. In addition to these scales, electrophysiological methods like electromyography (EMG) and electroencephalography (EEG) are crucial for understanding the neural mechanisms underlying dystonia by measuring muscle and brain activity [8]. Imaging techniques such as functional MRI (fMRI) and positron emission tomography (PET) further contribute by revealing brain activity and structural changes associated with the disorder [9].

Recent advancements emphasize the importance of kinematic analysis, utilizing motion capture systems and inertial measurement units (IMUs) to provide quantitative assessments of movement patterns. These systems offer objective data on joint angles, velocity, and acceleration, aiding in the detection of motor function abnormalities [10]. The application of machine learning and artificial intelligence to analyze large datasets from these systems is also on the rise. These advanced methods enable the identification of subtle movement patterns that may not be visible to the human eye, thus enhancing diagnostic precision [11].

### **Gait analysis**

Gait analysis is a pivotal area of research in understanding dystonia, as walking is a complex motor task that reveals the functional impact of the disorder. Motion capture systems, such as Vicon or OptiTrack, capture detailed motion data by tracking markers placed on the patient's body, providing a three-dimensional representation of the gait cycle [12]. Wearable sensors, including IMUs, measure accelerations and angular velocities during walking, offering continuous monitoring useful for real-world assessments [13]. Key features extracted from gait data—such as stride length, cadence, gait velocity, joint angles, and variability—help differentiate between dystonic and non-dystonic gait patterns [14]. Machine learning algorithms, including Support Vector Machines (SVM)

and deep learning models, are employed to classify these gait patterns with high accuracy [15].

### **Freezing of gait (FoG)**

Freezing of gait (FoG), characterized by a sudden, temporary inability to move the feet despite the intention to walk, can also occur in dystonia. Detection methods for FoG often use wearable sensors to monitor gait parameters, identifying episodes through sudden changes in stride length and cadence [16]. Analysis of data from accelerometers and gyroscopes focuses on the frequency components of movement to detect characteristic FoG patterns [17]. Additionally, intervention strategies such as real-time auditory or visual cues are being explored to help patients overcome FoG episodes [18].

### **Postural instability**

Postural instability, a common issue in dystonia that increases the risk of falls and reduces mobility, is typically assessed using clinical tests like the Berg Balance Scale (BBS) and the Timed Up and Go (TUG) test [19]. These tests provide qualitative measures of balance and postural control. Force plates are another tool used to measure the center of pressure (CoP) during standing and dynamic tasks, with parameters such as sway velocity and path length analyzed to assess balance control [20]. Wearable sensors like IMUs offer additional insights by providing data on trunk sway and other body movements during standing and walking tasks [21]. Features such as sway amplitude, velocity, and frequency extracted from sensor data are then used by machine learning models to classify the severity of postural instability, aiding in the development of targeted interventions [22].

The state of the art in dystonia assessment is advancing towards more objective, quantitative measures through the integration of motion capture systems, wearable sensors, and machine learning algorithms. Assessments of gait, freezing of gait, and postural instability are critical in providing detailed insights into the motor impairments associated with dystonia. These technological advancements not only enhance diagnostic accuracy but also facilitate the monitoring of disease progression and the evaluation of therapeutic interventions.



## 3. Materials and methods

The data used in this study were collected in a controlled laboratory environment equipped with specific IMU sensors and supervised by a clinician who assessed patients using the UPDRS scale. This data collection was conducted over several years, allowing for the observation of disease progression in the patients.

Two primary software applications were employed for different purposes:

- **XSens MVN Analyze:** this software was used for processing the kinematic data collected by the IMU sensors and provided real-time visual feedback via an avatar that mirrored the patient's movements. Additionally, it was instrumental in segmenting the data according to different tasks during preprocessing.
- **Python 3.12.2:** this programming language was utilized for the comprehensive analysis of the collected data.

### 3.1 Materials and experimental set up

The research followed the principles outlined in the Declaration of Helsinki, and all participants provided written informed consent, which included permission for video recordings. Ethical approval was obtained from the Mass General Brigham research ethics committee and the Institutional Review Board at Jose Reyes Hospital in Manila, Philippines. The study began in October 2022 when the Philippines Collaborative Center for X-Linked Dystonia Parkinsonism (CCXDP) research team, working with Dr. Christopher Stephen, started their involvement. After training at the Motion Lab Analysis (MAL) and acquiring motion sensors, the team initiated data collection with participants in Roxas City, Panay Island. In February 2023, Dr. Stephen visited the Philippines for research and training, further enhancing the exchange of knowledge and expertise.

The data collection on XDP patients is ongoing, demonstrating the continuous commitment and progress of the research project. Data collection involved capturing kinematic data using Inertial Measurement Unit (IMU) sensors and video recordings. To analyze motion

kinematics, XSens Movella Awinda motion sensors were employed, providing detailed and precise representations of participants' movements and then Python 3.12.2 was used for the data analysis. The dataset comprises kinematic signals recorded during various tasks involving both lower and upper limbs. It is important to note that this data was collected in a laboratory setting, which may differ from a natural or home environment.

### 3.1.1 IMU sensors

Inertial Measurement Units (IMUs) are sophisticated sensors that provide critical data for measuring motion, capturing acceleration, angular velocity, and often magnetic field strength and atmospheric pressure. Typically, an IMU includes an accelerometer, gyroscope, and magnetometer, each measuring along three orthogonal axes [23].

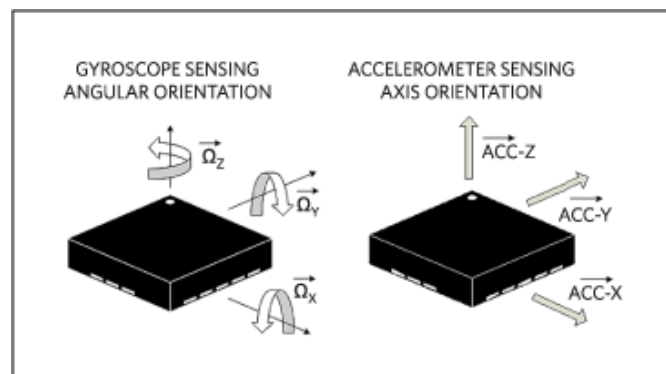


**Figure 3.1:** IMUs sensor

#### Accelerometers

Accelerometers are devices that measure the specific force of acceleration in one or more directions. They consist of a mass suspended by springs within a casing. When acceleration occurs, the mass moves, and this movement is measured by the changes in capacitance, piezoelectric properties, or other phenomena depending on the type of accelerometer. These changes are then converted into electrical signals that can be quantified to determine the magnitude and direction of the acceleration [23].

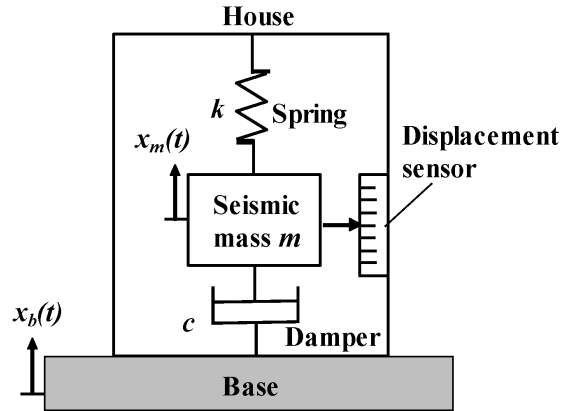


Figure 3.2: Accelerometer electrical circuit

### Gyroscopes

Gyroscopes measure the rate of rotation around a particular axis. They often use the principle of angular momentum to maintain orientation. In a MEMS gyroscope, a vibrating structure detects changes in orientation due to Coriolis forces acting on the vibrating mass. The amount of displacement caused by these forces is proportional to the rate of rotation, which is then converted into an electrical signal. Gyroscopes are crucial for applications requiring precise orientation and stabilization, such as in smartphones, drones, and gaming controllers [23].

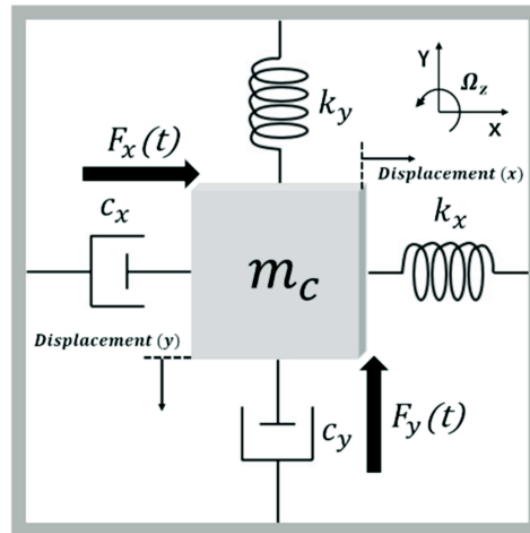
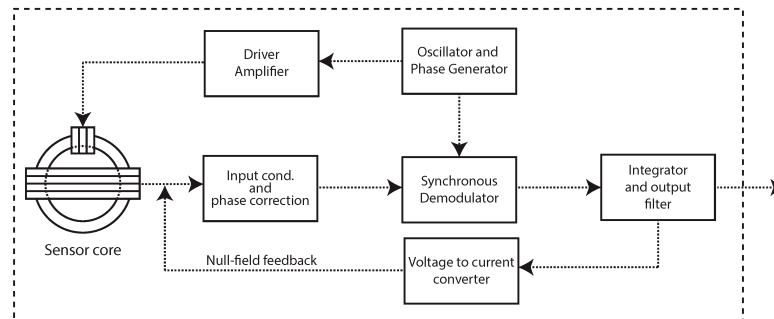


Figure 3.3: Gyroscope electrical circuit

## Magnetometers

Magnetometers measure the strength and direction of magnetic fields. They operate using various principles, including Hall effect sensors, fluxgates, or magneto-resistive technologies. By measuring the Earth's magnetic field, magnetometers can determine orientation relative to the magnetic north, which is essential for navigation systems. When combined with accelerometers and gyroscopes in an IMU, magnetometers help provide a complete picture of an object's orientation and movement [23].



**Figure 3.4:** Magnetometer circuit

The core technology behind modern IMUs is Micro Electro Mechanical Systems (MEMS), which integrate miniature mechanical and electronic components on a single chip. MEMS technology has made IMUs compact, efficient, and cost-effective, facilitating their widespread use in mobile devices, automotive systems, and aerospace applications. From an engineering standpoint, IMUs are essential for precise motion tracking and navigation. They are extensively used in environments where GPS is unreliable, such as underwater or space. The key challenge with IMUs is the accumulation of errors over time, known as drift. This occurs because the integration of small measurement errors over time leads to significant deviations in calculated positions and orientations. To mitigate this, IMUs are often used in conjunction with GPS and other sensors, utilizing sensor fusion algorithms like the Kalman filter to improve accuracy and reliability. Sensor fusion is a critical process in improving the performance of IMUs. It involves combining data from multiple sensors to produce more accurate and reliable information. This technique leverages the strengths of different sensors to compensate for their individual weaknesses. For example,

while accelerometers provide precise linear acceleration data, they are prone to noise; gyroscopes offer accurate rotational data but can drift over time. By fusing these data streams, a comprehensive and accurate representation of motion and orientation can be achieved [23, 24].

### Kalman filter

One of the most common algorithms used in sensor fusion is the Kalman filter, which operates in two main steps: prediction and update.

1. **Initialization:** the process begins with initial estimates of the state variables and their uncertainties.
2. **Prediction:** the state and covariance predictions are made based on the previous state and a model of the system's dynamics [25].
3. **Update:** new measurements are used to update the state estimates and reduce uncertainties through the calculation of the Kalman gain, followed by state and covariance updates [23].

This iterative process allows the Kalman filter to provide accurate state estimates even in the presence of noise and uncertainty, making it essential for applications requiring precise motion tracking.

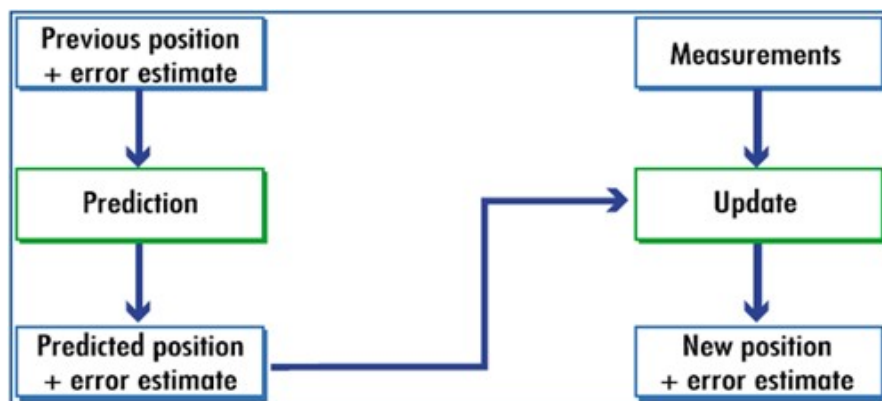


**Figure 3.5:** Flowchart of the Kalman filter process

In human activity recognition (HAR), IMUs are instrumental by capturing detailed motion data. These sensors can be placed on various body parts to monitor and classify activities such as walking, running, and sitting. The data are processed using machine learning algorithms to identify patterns and predict future activities. For instance, wearable

exoskeleton robots utilize IMUs to enhance control and assist users in daily tasks with high accuracy and low latency. IMUs also play a crucial role in rehabilitation, tracking patient progress and providing real-time feedback for therapeutic exercises [24, 26].

### 3.1.2 Xsens

The XSens 9-axis Inertial Measurement Units (IMUs) have been used in this study to collect data on body movements. These sensors measure acceleration, angular velocity, magnetic fields, and atmospheric pressure. The data were processed using MVN Software, which employs advanced algorithms and biomechanical models to accurately reconstruct the wearer’s movements in real-time.

The Xsens MVN system is an advanced motion capture solution for tracking full-body human motion. It combines miniature inertial sensors, wireless communication, and sophisticated sensor fusion algorithms. Its portability and versatility allow it to be used in various environments, including outdoors, offices, and workspaces, without needing to be confined to a studio or lab.

Figure	Description																		
 <p>Figure 33: MTw side view</p>	<p>The motion trackers are provided with a code indicating segment position.                      'L' or 'R': left or right side of the body.                      Segment: An abbreviation of the segment name.</p>																		
 <p>Figure 34: Full body strap set</p>	<p>While the straps are not labelled, the dimensions give an indication of their intended locations.</p> <table border="1"> <thead> <tr> <th>Segment</th> <th>Width (cm)</th> <th>Length (cm)</th> </tr> </thead> <tbody> <tr> <td>Pelvis</td> <td>10</td> <td>140</td> </tr> <tr> <td>Upper Leg</td> <td>10</td> <td>72</td> </tr> <tr> <td>Lower Leg</td> <td>5</td> <td>55</td> </tr> <tr> <td>Upper Arm</td> <td>5</td> <td>55</td> </tr> <tr> <td>Forearm</td> <td>5</td> <td>30</td> </tr> </tbody> </table>	Segment	Width (cm)	Length (cm)	Pelvis	10	140	Upper Leg	10	72	Lower Leg	5	55	Upper Arm	5	55	Forearm	5	30
Segment	Width (cm)	Length (cm)																	
Pelvis	10	140																	
Upper Leg	10	72																	
Lower Leg	5	55																	
Upper Arm	5	55																	
Forearm	5	30																	

**Figure 3.6:** Awinda full body strap set

The key components and functionalities of this system could be divided into hardware and software section:

#### Hardware Components

- Motion Trackers (MTx and MTx-STR): sophisticated IMUs with 3D accelerometers, gyroscopes, magnetometers, and barometers,

placed on key body parts.

- Body Pack (BP): central hub for data synchronization and transmission, powered by a rechargeable battery with up to 9.5 hours of recording time.
- Access Point (AP): manages data transmission between the Body Pack and the computer, supporting multiple systems.
- MVN Awinda System: wireless motion trackers (MTw) with internal batteries, using the Awinda Station and Dongle for data reception and synchronization.

### **Software and functionalities**

the MVN system is controlled via the MVN Analyze/Animate software a powerful windows 10 application for real-time motion capture, recording, and data analysis. It includes tools for calibration, live monitoring, playback, editing, and exporting data in various formats for integration with other software.

Xsens sensors were strategically placed on specific anatomical locations, including the head, trunk, shoulders, upper and lower arms, hands, pelvis, upper and lower legs, and feet, as depicted figure 3.7. The data collected from each sensor included the following parameters:

- a. Sensor Orientation
- b. Sensor Magnetic Field
- c. Sensor Free Acceleration
- d. Segment Velocity
- e. Segment Acceleration
- f. Segment Joint Angles
- g. Segment Angular Velocity
- h. Segment Angular Acceleration
- i. Segment Position

j. Center of Mass



**Figure 3.7:** Full body sensor displacement

Instead the Xsens Metaglove, created by Manus, utilizes precise finger tracking with sub-millimeter accuracy, seamlessly integrated into the Xsens motion capture system. This setup provided comprehensive finger-related data, particularly for the 3D position:

- Carpus
- Metacarpus
- Proximal, Middle, and Distal Phalanx

## 3.2 Data collection

The data collection process was supervised by Dr. Stephen and his team. It began with a clinical assessment to determine participant eligibility. Once eligibility was confirmed, the XSens motion sensors were set up. Participants were then instructed to perform a series of exercises to facilitate data collection.

### 3.2.1 Subjects

This diverse sample, encompassing participants from both North America and the Philippines, offers a comprehensive view of X-linked dystonia parkinsonism (XDP). Including individuals from various geographic regions enhances the dataset by incorporating potential differences in

genetic backgrounds, environmental influences, and healthcare access. This expands the study’s scope, enabling a more detailed understanding of XDP and allowing for the investigation of regional variations in the disease’s manifestation.

Our dataset is divided into baseline and follow-up data:

- **Baseline Data:** this includes 37 subjects from both the U.S. cohort and Panay Island. Specifically, from the U.S. cohort, we have 3 manifest male XDP cases, 1 at-risk male, 5 symptomatic carrier females, and 5 control individuals with baseline data only. From Panay Island, there are 24 subjects, consisting of 23 manifest male cases and 1 carrier female.
- **Follow-up Data:** this section involves only Filipino subjects who participated in follow-up data collections to track disease progression, totaling 20 subjects. The follow-up data is further divided into two groups:
  - a. 6-month Follow-Up: includes 12 manifest male cases and 1 carrier female.
  - b. 12-month Follow-Up: comprises 6 manifest male cases and 1 carrier female.

Overall, the dataset consists of 57 subjects as shown in the figure below (Figure 3.8).

	MALES	FEMALES	
XDP	26 (23 Filipinos)	6 (1 Filipinos)	37
CONTROLS	3	2	
6 MONTHS FOLLOW-UP (Filipinos)	12	1	20
12 MONTHS FOLLOW-UP (Filipinos)	6	1	

**Figure 3.8:** Subjects involved in the study.

The following tables aim to display the age, age at onset, and gender of each participant in our study for both baseline (Figure 3.9) and follow-up (Figure 3.10).

### 3.2. DATA COLLECTION

Subject	Age	Age at the Onset	Gender
P-2019-0671	44	36	Male
P-2022-0767	59	42	Male
P-2022-0766	57	N.A.	Female
P-2014-0207	51	38	Male
P-2014-0210	18	N.A.	Male
P-2014-0205	71	N.A.	Female
P-2015-0276	52	N.A.	Female
P-2022-0768	78	N.A.	Female
P-2022-0769	53	N.A.	Female
Q-2023-0586	53	50	Male
Q-2018-0313	64	49	Male
Q-2018-0312	52	38	Male
Q-2021-0510	46	43	Male
Q-2023-0587	56	51	Female
Q-2023-0588	30	26	Male
Q-2020-0479	39	29	Male
Q-2020-0478	36	N.A.	Male
Q-2023-0589	58	47	Male
Q-2023-0590	53	49	Male
Q-2023-0591	49	N.A.	Male
Q-2023-0592	49	40	Male
Q-2023-0593	44	29	Male
Q-2023-0594	34	32	Male
Q-2020-0461	52	44	Male
Q-2023-0599	59	47	Male
Q-2023-0600	62	52	Male
Q-2023-0653	44	43	Male
Q-2023-0654	33	N.A.	Male
Q-2024-0682	52	47	Male
Q-2024-0683	65	50	Male
Q-2024-0685	44	37	Male
Q-2024-0686	35	N.A.	Male
P-2016-0482	29	N.A.	Female
P-2016-0483	56	N.A.	Female
P-2016-0484	57	N.A.	Male
P-2016-0481	21	12	Male
P-2023-0794	29	N.A.	Male

XDP PATIENTS

CONTROLS

**Figure 3.9:** Baseline set: demographic information.

Subject	Age	Age at the Onset	Gender	
Q-2023-0586	53	50	Male	6-MONTHS FOLLOW-UP
Q-2018-0313	64	49	Male	
Q-2018-0312	52	38	Male	
Q-2021-0510	46	43	Male	
Q-2023-0587	56	51	Female	
Q-2023-0588	30	26	Male	
Q-2020-0479	39	29	Male	
Q-2020-0478	36	N.A.	Male	
Q-2023-0589	58	47	Male	
Q-2023-0590	53	49	Male	
Q-2023-0591	49	N.A.	Male	
Q-2023-0592	49	40	Male	
Q-2020-0461	52	44	Male	
Q-2020-0478	36	N.A.	Male	12-MONTHS FOLLOW-UP
Q-2020-0479	39	29	Male	
Q-2021-0510	46	43	Male	
Q-2023-0589	58	47	Male	
Q-2023-0588	30	26	Male	
Q-2023-0590	53	49	Male	
Q-2023-0592	49	40	Male	

**Figure 3.10:** Follow-up set: demographic information.

Looking at the baseline dataset, noteworthy demographic difference emerges among the groups studied:

- Control group: mean age of 38.4, ranging from 21 to 57
- XDP patients: mean age of 47.65, ranging from 18 to 78

These findings highlight the diverse age distributions within each group, offering valuable insights into the age-related characteristics of XDP and control participants.

### 3.2.2 Tasks and UPDRS scale

The study involved 24 tasks designed to provoke dystonia, categorized into five primary groups:

1. **Upper limb tasks:** finger tapping, hand movement (opening/-closing), pronation/supination, finger to Nose.

2. **Lower limb tasks:** leg agility, toe tap, heel/toe alternating movement.
3. **Head tasks:** turning head, ear to shoulder.
4. **Resting tasks:** seated with palms down, seated with palms up, seated with eyes closed, seated while reciting the months of the year backward, wing-beating position, arms outstretched with eyes open and closed.
5. **Gait tasks:** arise from chair, trunk and posture, walking, turning, walking on toes, tandem gait, backward walking, retropulsion Ppll.

This classification enables a detailed analysis of dystonia-related patterns and features across various motor functions, offering a thorough understanding of how X-linked dystonia-parkinsonism affects both upper and lower limbs as well as gait.

All tasks were evaluated by a single experienced clinician and the use of a comprehensive array of rating scales, including the Blepharospasm Scale, Unified Parkinson's Disease Rating Scale (UPDRS), XDP Rating Scale, Toronto Western Spasmodic Torticollis Rating Scale (TWSTRS), and the Tsui Torticollis Scale, ensures an extensive evaluation of various aspects related to dystonia and associated movement disorders. Each of these scales is designed to measure specific elements of motor function and symptom severity, collectively offering a detailed understanding of the participants' conditions.

Specifically, for the purpose of this study, the patients' scores on the UPDRS were utilized.

### **Unified Parkinson's Disease Rating Scale (UPDRS)**

The Unified Parkinson's Disease Rating Scale (UPDRS) is a widely recognized tool for evaluating the severity of Parkinson's disease and tracking its progression. Initially developed in the 1980s, the UPDRS has undergone several revisions and updates. The scale is divided into multiple parts, each addressing different aspects of Parkinson's disease:

- **Part I:** non-motor experiences of daily living - this section includes thirteen items, split into six items for rater-based assessment

(evaluated by clinicians or researchers) and seven items for patient self-assessment.

- **Part II:** motor experiences of daily living - comprising 13 items based on patient self-reporting.
- **Part III:** motor examination - consisting of 18 items evaluated by the clinician.
- **Part IV:** motor complications - including six items focused specifically on dyskinesia and fluctuations. A trained clinician administers the UPDRS through patient interviews and observation of both motor and non-motor symptoms. The disease's severity is assessed based on the clinician's expertise. Each part is scored separately from 0 (healthy) to 4 (severe), and the total score offers an overall evaluation of the impact of Parkinson's disease.

In this research, we specifically chose the Unified Parkinson's Disease Rating Scale as the sole assessment tool for creating the label vector in our supervised learning algorithm. This choice was made to enhance the model's reliability and specificity, as the UPDRS provides a comprehensive overview of the clinical manifestations of Parkinson's disease, thereby contributing to the robustness of our analytical framework.



## 3.3 Methods

For this study, the analysis concentrated on three specific tasks, following the criteria from the Unified Parkinson's Disease Rating Scale (UPDRS):

### 1. Gait task

This task allows the examiner to make a simultaneous observation of both sides of the body, like the movement coordination, and to detect subtle signs of motor dysfunction that might indicate the presence of dystonia or parkinsonism, providing insight into the severity and progression of the disorder. The patients are asked to walk away from and then towards the clinician for at least 10 meters (30 feet), turn around, and return to the examiner.

### 2. Freezing of gait (FoG) task

The freezing of gait is a common and disabling symptom, particularly in advanced stages of movement disorders like Parkinson's disease and dystonia. It is characterized by the sudden, temporary inability to move the feet forward despite the intention to walk. The assessment of the freezing of gait while is a crucial point in the XDP evaluation. Indeed, this procedure helps distinguish between different movement disorders and could give important information about how fluid and coordinated is the walk, especially during turns.

### 3. Postural instability task

Postural instability involves assessing how well a patient can maintain their balance, especially when subjected to sudden movements or displacements. In dystonia and related disorders, balance control is often impaired, increasing the risk of falls. Evaluating postural stability helps clinicians understand the degree of motor control loss and the potential need for supportive therapies to prevent falls and enhance patient safety. These evaluations are critical for several reasons:

- Diagnostic accuracy: they help distinguish dystonia from other neurodegenerative disorders that might have overlapping symptoms.
- Monitoring progression: regular assessments can track how the disease evolves over time, allowing for adjustments in treatment plans.
- Treatment effectiveness: they provide a baseline to measure the effectiveness of interventions and therapies.

This test evaluates the patient's response to a sudden displacement by pulling the shoulders while they stand upright with eyes open and feet parallel. The examiner stands behind the patient, explains the procedure, and allows the patient to step backward to prevent falling. After an initial mild and unrated pull for demonstration, a second forceful pull is performed to shift the patient's center of gravity, requiring them to step backward. The examiner observes the number of steps taken or if the patient falls.

As outlined in the previous chapter, our data collection methodology involves gathering two types of data: kinematic data (collected by using XSens Movella Awinda motion sensors) and video recordings (through the use of cameras).

In this study, we exclusively used motion sensor data, while video recordings were solely for scoring purposes. This approach allows us to focus on the objective and quantifiable data provided by the motion sensors, ensuring a thorough examination of biomechanical aspects without the potential biases of subjective video assessments. This reliance on motion sensor data supports our goal of developing an automated assessment tool for X-linked dystonia-parkinsonism, highlighting the need for objective diagnostic tools that can be used in various settings, including remote areas with limited access to specialized medical expertise.

#### **Project pipeline**

The project pipeline (Figure 3.11), developed in Python 3.12.2, consists of several key steps:

- Pre-processing

- Gait events and spatio-temporal parameters evaluation or windowing
- Feature extraction
- Feature selection and feature projection
- Classification

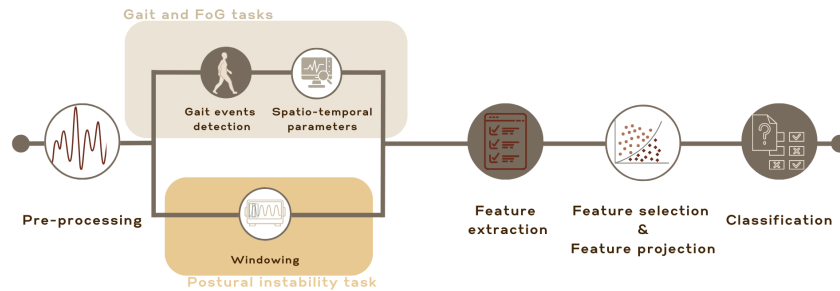


**Figure 3.11:** Project pipeline

This section delineates the methodologies used at each stage of the pipeline, providing a detailed explanation of the techniques employed at each point. Furthermore, the rationale and significance behind each technique are elaborated upon, enhancing the overall transparency and interpretability of the experimental process.

### 3.3.1 Pre-processing

Data preprocessing is a critical phase in the data analysis pipeline, transforming raw data into a structured format suitable for analysis. The quality of preprocessing directly impacts the accuracy and effectiveness of subsequent analyses, as raw datasets often contain errors, missing values, outliers, and inconsistencies that must be addressed to extract meaningful insights. Effective preprocessing techniques are vital in medical informatics to address data imperfections, leading to more accurate and reliable results. This aligns with our approach to preprocessing, ensuring the data's suitability for detailed analysis [27].

In this study, the data from XSens Movella Awinda motion sensors underwent preprocessing using MVN Analyze software. This step was essential to ensure the cleanliness and reliability of the data. A biomechanical model was applied to further refine the data. Given the inherent reliability of the data post-MVN Analyze preprocessing,

additional filtering was not performed. Instead, the preprocessing phase focused solely on segmenting the data for analysis. Using inertial sensing technology like XSens MVN provides consistent and reliable tracking of human motion. This supports our reliance on high-quality motion sensor data, reinforcing the decision to use the preprocessed data from MVN Analyze without further filtering [28].

In our study, min-max normalization was applied to each feature to ensure that the evaluations of signals were comparable across different subjects. This preprocessing step was critical for achieving consistent and reliable results when classifying patients into different clinical categories.

### Min-max normalization

Min-max normalization is a widely used technique in data preprocessing for machine learning. It scales the data to a specific range, typically [0, 1], by transforming each feature using the formula:

$$X_{\text{normalized}} = \frac{X - X_{\min}}{X_{\max} - X_{\min}}$$

This process ensures that all features contribute equally to the model's performance and helps improve the convergence of optimization algorithms, particularly those that are sensitive to the scale of input features, such as gradient descent [29, 30].

To evaluate the various tasks, different types of signals were used:

- **Gait task:** feet position, feet velocity and acceleration, vertical angular velocity of feet and forearms and several joint angles signals (ankles dorsi/plantarflexion, knees flexo/extension and internal/external rotation).
- **Freezing of gait task:** linear pelvis acceleration, feet position, feet velocity and acceleration, vertical angular velocity of feet, forearms and pelvis and several joint angles signals (ankles dorsi/plantarflexion, knees flexo/extension and internal/external rotation).
- **Postural instability task:** linear pelvis acceleration, antero-posterior pelvis acceleration, feet position, feet velocity and acceleration, vertical angular velocity of feet, forearms and pelvis and several joint angles signals (ankles dorsi/plantarflexion, knees flexo/extension).

### 3.3.2 Gait analysis

For the gait analysis, prior to detecting individual events such as strike and toe-off, we initially identified the turning points in the patients' gait. Throughout the duration of the gait task, patients walk straight and then make a certain number of turns. To detect these curves, we utilized vertical angular velocity and applied filtering exclusively to this signal. Specifically, we filtered the signal with a cutoff frequency of 1 Hz and analyzed zero-crossings to determine the beginning and end of each turn.

After identifying the curves, we proceeded with the detection of strike and toe-off events. For this, we primarily used the linear acceleration of the pelvis and joint angle signals of the feet, focusing on the dorsiflexion and plantarflexion of both the right and left feet. This dual detection approach was chosen because literature suggests that pelvic acceleration is the gold standard for detecting strike and toe-off events. However, due to the cleaner signal obtained from the ankle joints, we initially performed the detection on these joint angle signals (Figure 3.12) before proceeding with the pelvic linear acceleration (Figure 3.13).

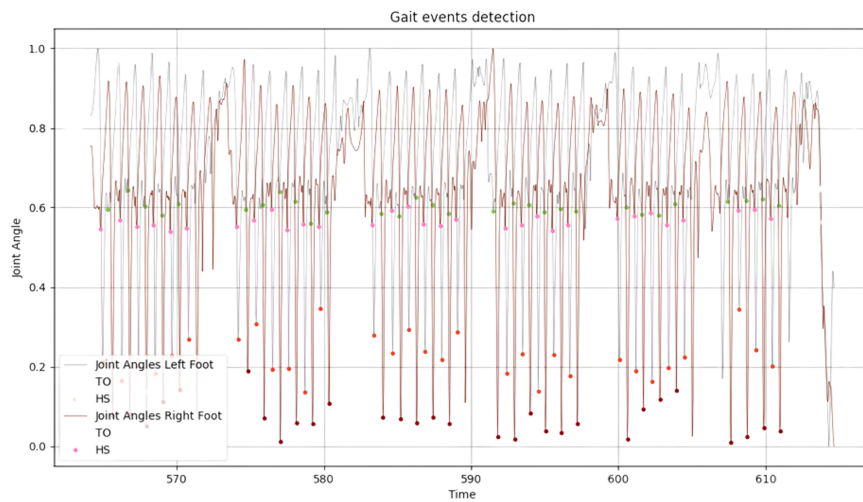


**Figure 3.12:** Gait events detection on ankles

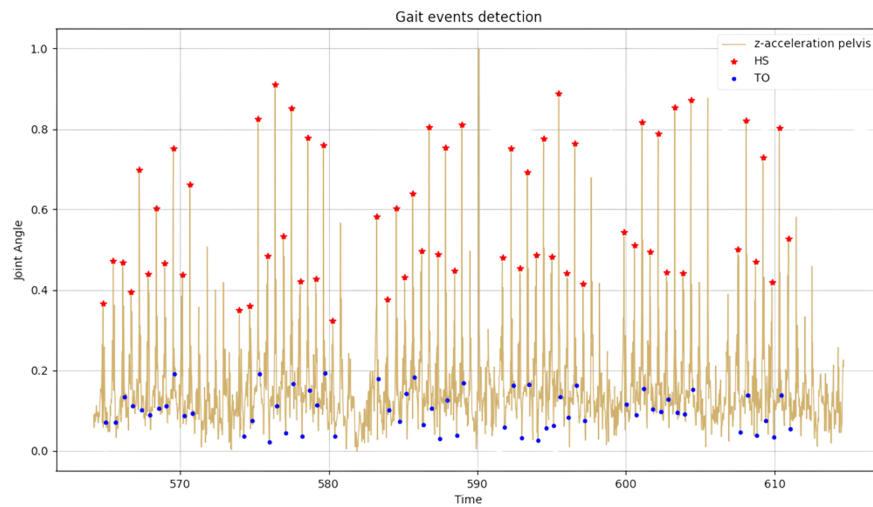


**Figure 3.13:** Gait events detection on pelvis

We then matched the events detected from both the pelvis and the feet, finding an almost perfect alignment between them (Figure 3.14).

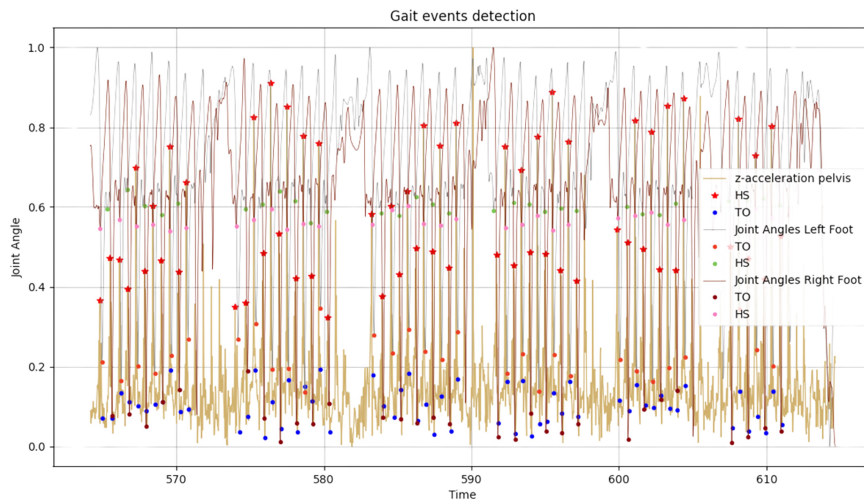


**Figure 3.14:** Gait events detection match

This dual detection method was essential not only for calculating features individually for both sides of the body but also for some features that required signals from the pelvis or trunk.

### Spatio-temporal parameters

After identifying the gait events, specifically strike and toe-off, this foundational step was crucial for calculating the spatiotemporal parameters of gait (Figure 3.15).

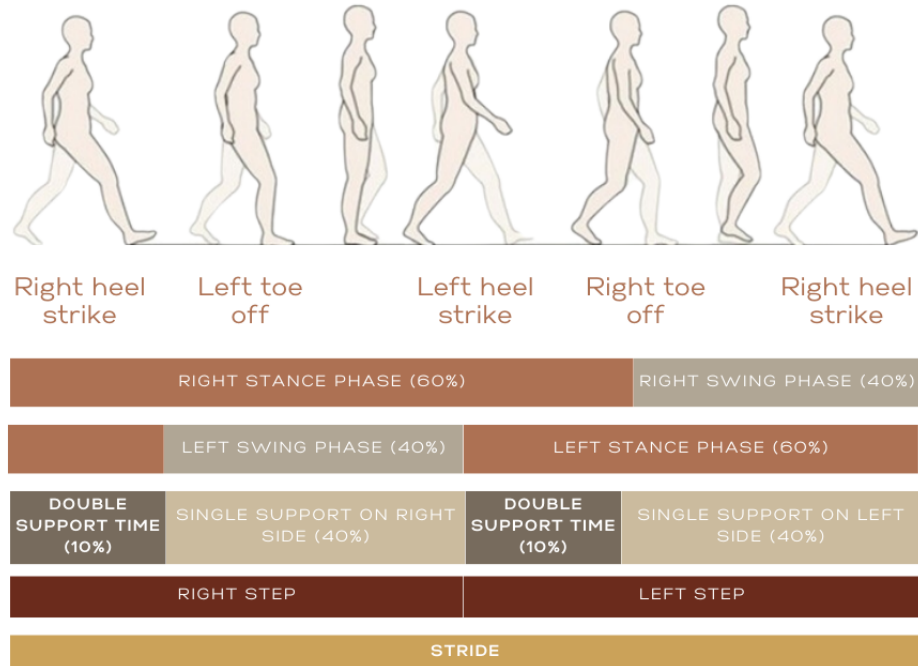


**Figure 3.15:** Gait parameters

These parameters are essential for data analysis as they play a vital role in assessing and differentiating the severity of the disease among patients. For example, stride length is a critical feature in distinguishing the severity of the condition, making the calculation of these parameters essential. As depicted in the figure below, the key spatiotemporal parameters include stride, stance, step, swing, double support time, single support time, and cadence (Figure 3.16).

Stride/ stride time
Stance/ stance time
Step/ step time
Swing/ swing time
Double support time
Single support time
Cadence

**Figure 3.16:** Spatio-temporal parameters

The computation of these parameters is also vital because certain features need to be derived from specific gait events, such as swing or stride, as we will discuss later.

### 3.3.3 Feature extraction and dataset construction

Feature extraction is a crucial process in data analysis, especially in the context of AI projects for clinical data. Studies have demonstrated that effective feature extraction significantly enhances the accuracy and reliability of predictive models. For example, a framework for feature extraction from hospital medical data has been developed to support risk prediction tasks. This approach allows for the creation of rich, data-driven feature sets that improve the performance of machine learning models in predicting patient outcomes and other clinical tasks [31].

The aim of feature extraction in this study was to identify and isolate significant task-specific features, guided by clinical observations. This method ensured that the chosen features were both relevant to the tasks and aligned with clinical insights, improving their interpretability and clinical relevance. Integrating clinical expertise into the feature extraction process enhances the robustness and validity of the data analysis.

#### Gait task

The feature evaluation was conducted on both sides, drawing from prior clinical observations, resulting in a total of 93 features (Table 3.1).

<b>Feature</b>	<b>Clinical meaning</b>
<b>Gait speed</b>	bradykinesia[32]
<b>Dominant frequency</b>	rhythmicity of movement
<b>Stride length</b>	impaired locomotion[32, 33, 34]
<b>Dominant frequency/total energy</b>	
<b>Gait asymmetry index</b>	gait asymmetry[35]
<b>Min, max, std and variance</b>	
<b>Coefficient of variation (CV)</b>	step-to-step variability[36, 37, 38]
<b>Energy around the dominant frequency</b>	rhythmicity of movement
<b>Root mean square (RMS)</b>	bradykinesia
<b>Skewness and kurtosis</b>	
<b>Cross-correlation</b>	coordination of movement
<b>Amplitude of dominant frequency</b>	
<b>Range of motion (ROM)</b>	postural control[39]
<b>Step length</b>	impaired locomotion[32, 33, 34]

Table 3.1: Gait features table

### Freezing of gait task

As for the gait task, the feature evaluation was conducted on both sides, mainly on the turns segment, resulting in a total of 123 features. In particular, the number of features assessed for the gait task has been maintained while incorporating additional specific features relevant to the analysis. (Table 3.2).

<b>Feature[40]</b>
<b>Freezing index</b>
<b>Energy</b>
<b>Power</b>
<b>Power in freeze band</b>
<b>Power in locomotor band</b>

**Table 3.2:** Freezing of gait features table

Regarding the dataset construction for both gait and freezing of gait tasks, the features were calculated by segmenting the patient signals into multiple samples, corresponding to the number of straight paths they performed, with the same number of turns. The features were calculated based on each step, stride, or swing event, depending on the type of feature. This segmentation was necessary because some features need to be assessed during specific gait events, and thus, the application of the sliding windows technique was not as effective in providing useful information.

### Postural instability task

The feature evaluation was conducted bilaterally, based on prior clinical observations, resulting in a total of 88 features (Table 3.3). For the other two tasks, only the 'gait' signal segment was assessed. However, for the postural instability task, we focused on the 'retropulsion' test segment. During this segment, the clinician evaluated the number of backward steps taken by the patients to assign a score. Given the shortness of this segment and the limited number of steps, it was necessary to apply

the sliding windows technique with a window length of 1 second and a 80% overlap. Consequently, the dataset contains a higher number of samples per patient for the postural instability task compared to the other tasks.

<b>Features[41]</b>
<b>RMS</b>
<b>Jerk</b>
<b>F95</b>
<b>Length sway</b>
<b>Centroidal frequency</b>
<b>High frequency power</b>
<b>Mean velocity sway</b>
<b>Frequency dispersion</b>
<b>Sway area</b>
<b>Skewness, kurtosis</b>

**Table 3.3:** Postural instability features table

### 3.3.4 Feature selection

Feature selection is a fundamental process in data analysis, particularly when managing complex and high-dimensional datasets. This process enhances the efficiency and effectiveness of modeling algorithms by pinpointing and retaining only the most relevant features. By reducing the dimensionality of the data, the feature selection not only streamlines computational efforts but also improves model interpretability and predictive performance. The primary aim of feature selection is to identify and maintain a subset of features that significantly contribute to the specific task, while discarding irrelevant or redundant information [42].

This approach not only simplifies the computational process but also

aids in uncovering underlying patterns and relationships within the data, leading to more accurate and interpretable results. Effective feature selection can prevent overfitting and reduce model complexity, making it easier to deploy models in real-world applications.

Feature selection techniques can be categorized into three main types:

1. Filter methods: use statistical measures to evaluate the relevance of features independently of any learning algorithm. Techniques such as Pearson's correlation, Chi-square test, and mutual information are common examples.
2. Wrapper methods: involve selecting features based on the performance of a specific learning algorithm. Recursive Feature Elimination (RFE) is a popular wrapper method that recursively removes features and builds models to identify the optimal subset.
3. Embedded methods: perform feature selection during the model training process. Regularization techniques like Lasso and Ridge regression fall under this category, which add penalties to the model for complexity, thereby selecting features that contribute the most to prediction accuracy.

In this project pipeline, the Recursive Feature Elimination (RFE) method, which is part of the wrapper methods category, was employed in conjunction with a Random Forest classifier to enhance feature selection, combined with k-fold cross-validation to validate the model's performance reliably (Figure 3.17). Before implementing this procedure, the correlation between features in the initial dataset was calculated to ensure its reliability.



**Figure 3.17:** Feature selection pipeline

The process (figure 3.17) begins with the initial set of features, from which a correlation matrix is computed. This matrix is used to identify and eliminate features that have a correlation coefficient of 0.9 or higher, ensuring that highly similar features are removed. The reduced set of features is then subjected to Recursive Feature Elimination (RFE)

combined with k-fold cross-validation to assess the performance of a Random Forest classifier trained on this subset. The RFE process iteratively removes the least significant feature, starting with the full feature set and continuing until only one feature remains. Throughout this process, the F1 score is used to evaluate the performance of the model at each step. The goal is to find the smallest subset of features that allows the model to achieve at least 95% of the performance it would have with the complete feature set (after correlation-based elimination).

The following paragraphs will provide a detailed explanation of the techniques used.

### **Correlation between features**

In data analysis, particularly in the context of high-dimensional datasets, calculating the correlation between features is a critical step. This helps in identifying and eliminating redundant features, which can enhance model performance and interpretability. One effective approach to achieve this is through feature selection based on correlation. This method helps in identifying and eliminating redundant features that do not add significant value to the predictive modeling process. There are several methods to calculate correlation and apply feature elimination, including:

- a. Pearson correlation coefficient: it measures the linear correlation between two variables. Values range from -1 to 1, where 1 indicates a perfect positive linear relationship, -1 indicates a perfect negative linear relationship, and 0 indicates no linear relationship.
- b. Spearman's rank correlation: a non-parametric measure of rank correlation. Assesses how well the relationship between two variables can be described using a monotonic function. Useful when the data are not normally distributed or when dealing with ordinal variables.
- c. Kendall's tau correlation: another non-parametric measure of correlation. Useful for small sample sizes and ordinal data. Measures the strength and direction of association between two variables.

Among the various methods for correlation-based feature elimination, the Threshold-Based Feature Elimination is a widely used technique.

This method involves setting a predefined threshold for the correlation coefficient, above which features are considered redundant and are removed from the dataset. This helps in mitigating multicollinearity, reducing the complexity of the model, and improving its performance. This method is based on computing the correlation matrix of all features and setting a threshold to identify pairs of highly correlated features. Features that have a correlation coefficient above the set threshold are considered redundant and are removed. In this project, a threshold of **90%** was applied, meaning any features with a correlation coefficient of 0.9 or higher were eliminated to reduce multicollinearity and ensure the dataset's reliability.

#### Benefits of Threshold-Based Feature Elimination

1. Improved model performance: by removing highly correlated features, the model becomes less prone to overfitting and can generalize better to new data.
2. Enhanced interpretability: simplifying the model by reducing the number of features makes it easier to understand and interpret the relationships between the remaining features and the target variable.
3. Reduced computational cost: fewer features mean less computational resources are required for training the model, leading to faster processing times.

#### **Recursive Feature Elimination (RFE)**

Recursive Feature Elimination (RFE) is a powerful feature selection method used to enhance the performance of machine learning models by iteratively removing less important features. This technique helps in simplifying models, reducing overfitting, and improving the model's interpretability and accuracy [43].

This method is characterized by several steps:

1. **Model training:** the process begins by training a model using all available features. A common choice for the model in RFE is a linear model or a tree-based model, such as Random Forest or Support Vector Machines (SVM).

2. **Feature ranking:** once the model is trained, each feature is assigned an importance score based on its contribution to the prediction accuracy. In the context of tree-based models like Random Forest, this could be the decrease in impurity or the Gini index when a feature is used for splitting.
3. **Elimination:** the least important features are removed from the dataset. The number of features to remove at each iteration can be predetermined by the user. Typically, one or a small percentage of features are removed in each iteration to avoid losing important information prematurely
4. **Iteration:** the model is retrained with the remaining features, and the process of ranking and eliminating features is repeated. This iterative process continues until a specified number of features is reached or until the model performance stops improving.
5. **Optimal subset selection:** the subset of features that results in the best model performance is selected as the final feature set. The model trained on this optimal subset is then used for prediction.

### Random Forest classifier

The Random Forest Classifier is a widely-used ensemble learning algorithm specifically designed for classification tasks. It builds multiple decision trees during the training phase and then merges their outputs to generate more accurate and stable predictions. Developed by Leo Breiman, Random Forests have gained popularity due to their robustness, ease of use, and effectiveness in handling various types of data, including those with high dimensionality [44, 45].

One of the fundamental concepts of the Random Forest Classifier is the creation of an ensemble of decision trees. Each tree is trained on a different subset of the training data, which is generated through bootstrap sampling, a method that involves random sampling with replacement. This approach, known as bagging (Bootstrap Aggregating), introduces randomness into the data sampling process, which helps in reducing overfitting—a common issue in single decision trees [44].

At each node within a tree, a random subset of features is selected to find the best split for the data. This random feature selection ensures that the trees are diverse and less correlated, which leads to a more

robust and accurate model. By not considering all features at each split, the model avoids overfitting to specific features and gains generalizability across different datasets [44].

Each tree in the forest is grown to its maximum depth without pruning. This results in "deep" and complex trees. However, the ensemble approach mitigates the risk of overfitting. During training, the data is split at each node based on the best feature and threshold that maximize class separation, typically using criteria like Gini impurity or information gain [45].

Once all the trees have been trained, the Random Forest Classifier makes predictions for new data points by aggregating the predictions of individual trees. In classification tasks, each tree votes for a class, and the class with the majority vote is selected as the final prediction. This majority voting mechanism ensures that the overall model is less sensitive to the biases of individual trees, leading to more accurate and stable predictions [44].

A significant advantage of the Random Forest Classifier is its ability to measure feature importance. Feature importance is calculated based on the average decrease in Gini impurity (or another metric) caused by each feature across all trees in the forest. These importance scores help identify which features contribute most to the model's predictive performance, providing insights into the underlying structure of the data [46].

Random Forests are inherently capable of handling missing values and outliers effectively. Since each tree is built on a different subset of the data, the impact of missing values is minimized. Outliers are also less influential because the aggregation of multiple trees tends to decrease their effect [45].

#### Advantages:

- **Robustness:** the ensemble approach ensures robustness against overfitting and improves generalization to unseen data.
- **Versatility:** can handle both classification and regression tasks, though primarily discussed here in the context of classification.
- **Ease of use:** requires minimal parameter tuning compared to other machine learning algorithms.

- **Interpretability:** provides feature importance scores, offering insights into the data and the model.

### Cross Validation

Cross-validation is a crucial technique for evaluating the robustness and generalizability of machine learning models. This method involves partitioning the dataset into multiple subsets, known as folds, and systematically using these folds for both training and validation. By doing so, cross-validation provides a comprehensive assessment of a model's performance across different data subsets, reducing the risk of overfitting and offering a more realistic estimation of its effectiveness [47].

The primary goal of cross-validation is to provide a comprehensive evaluation of a model's performance. By systematically rotating through different subsets of the dataset, cross-validation offers insights into the model's ability to generalize to new, unseen data. This process is essential for making informed decisions about the model's suitability and reliability for real-world applications. Various cross-validation techniques can be tailored to the specific nature of the dataset, ensuring that the chosen method aligns with the characteristics and requirements of the data under investigation [48].

In this research, k-fold cross-validation and leave-one-group-out cross-validation were employed to evaluate model performance. The k-fold approach was specifically applied in the feature selection section, while the leave-one-group-out method was used for prediction of the score. These methods provided robust evaluations, ensuring that the models developed were both reliable and generalizable.

### K-Fold Cross-Validation

K-fold cross-validation is one of the most commonly used methods. In this approach, the dataset is divided into k equally sized folds. The model is trained on k-1 folds and validated on the remaining one fold. This process is repeated k times, ensuring that each fold serves as a validation set exactly once. For instance, in this study, a 10-fold cross-validation was adopted. This means the dataset was split into 10

parts, and the model was trained and validated 10 times, each time with a different fold held out for validation. This method provides a robust measure of model performance by averaging the results from all folds, thereby reducing variance and providing a more reliable estimate of the model's ability to generalize to unseen data [48].

### **Leave-One-Group-Out Cross-Validation**

Leave-one-group-out cross-validation is particularly useful when dealing with grouped or clustered data. In this technique, entire groups or sets of related observations are systematically excluded from the training and validation sets in each iteration. This ensures that the model is evaluated on its ability to generalize to completely unseen groups, which is crucial for ensuring robustness in real-world applications where data can exhibit grouping. In this study, the leave-one-group-out approach was applied by grouping data associated with individual subjects. This method helps mitigate potential overfitting by ensuring comprehensive evaluation across different subjects [49].

### **3.3.5 Feature projection**

The features identified through the feature selection pipeline were subsequently used to create visual projections within a reduced dimensionality feature space. This was achieved using the Sammon mapping technique, a nonlinear dimensionality reduction method that preserves the structure of the data as much as possible when reducing its dimensions. Sammon mapping is effective for visualizing high-dimensional data by maintaining the inter-point distances from the high-dimensional space in the lower-dimensional projection. This makes it a powerful tool for revealing underlying patterns and relationships within the data, enhancing the interpretability of the feature space [50, 51].

The color-coded projections generated through Sammon mapping provided valuable insights into how selected features relate to different clinical categories. By highlighting these relationships, the projections facilitated a more intuitive understanding of the data, making it easier to interpret and analyze the results [52].

### Sammon mapping plot

Sammon mapping projections provide an effective visual representation of high-dimensional data within a reduced-dimensional space. This technique aims to preserve the pairwise dissimilarities or distances between data points, enabling a clearer visualization of the dataset's inherent structure. By maintaining these relationships, Sammon mapping facilitates an intuitive understanding of complex data patterns and clusters.

In our study, we generated 3D Sammon mapping projections using the ten features identified as most important by the Random Forest Regressor. These features were deemed crucial by the regression model and are central to shaping the visual representation of the data in the reduced-dimensional space. The projections are color-coded to enhance interpretability, highlighting clusters corresponding to different clinical labels. This approach allows for an insightful exploration of relationships between features and clinical categories, aiding in the discovery of intricate patterns and providing a deeper understanding of the data's underlying structure [50, 51, 52].

#### 3.3.6 Classification

Using the fine-tuned Random Forest Regressors, clinical labels were derived to achieve the goal of this study. Specifically, the project aimed to classify patients into three distinct categories. By employing this method with with Leave-one-Out cross-validation algorithm, we were able to accurately differentiate among the three classes of patients, ensuring precise and reliable classification results.

#### Random Forrest Regressor

The Random Forest Regressor is a robust and versatile ensemble learning method used extensively for regression tasks. This technique builds multiple decision trees, each trained on different subsets of the data and a random selection of features, a process known as bootstrap aggregating or bagging. By averaging the predictions of these trees, the Random Forest Regressor achieves high predictive accuracy and reduces the risk of overfitting. This ensemble approach also enhances the model's ability to generalize from the training data to unseen datasets, making it particularly effective in handling complex, high-dimensional data [44,

53, 54].

Key aspects of the Random Forest Regressor include its ability to estimate feature importance, which helps identify the most influential variables in the dataset. This is particularly useful in reducing dimensionality and improving model interpretability. Additionally, the method is known for its resilience to overfitting, especially when compared to single decision trees, due to the randomness introduced in both the data sampling and feature selection processes [44].

In the context of this study, the Random Forest Regressor was employed with leave-one-out cross-validation (LOO-CV) to predict scores in three distinct tasks. LOO-CV is a rigorous validation technique where each data point is used once as a test case while the remaining points form the training set. This method provides an unbiased estimate of model performance, particularly valuable in medical and clinical research where data points (patients) are often few but highly significant [53].

## 4. Results and discussion

The subsequent sections delve into the findings of our study, detailing the results of the machine learning algorithms used to achieve our research objectives (Aim1:assess the presence and gravity of the disease, Aim2:assess the disease progression in patients). For each task, we will present Sammon mapping projections, derived from selecting the most significant features as previously described. This qualitative analysis aims to shed light on the model's performance. Furthermore, we will provide confusion matrices for the optimized Random Forest Regressor, offering a quantitative evaluation of the achieved accuracies and F1 scores in our study.

### 4.1 Gait task

For the gait task, as explained in the previous chapter, the features were evaluated based on the gait events detected during the gait analysis.

Given the large number of features and the possibility of redundant information, a feature selection algorithm was applied before proceeding with the prediction of the score.

#### 4.1.1 Feature projection

After evaluating the correlation matrix between features, 21 features were removed from the initial set of 93 due to the presence of 42 similar features. Following the application of the feature selection algorithm, only 11 features were ultimately selected for further analysis.

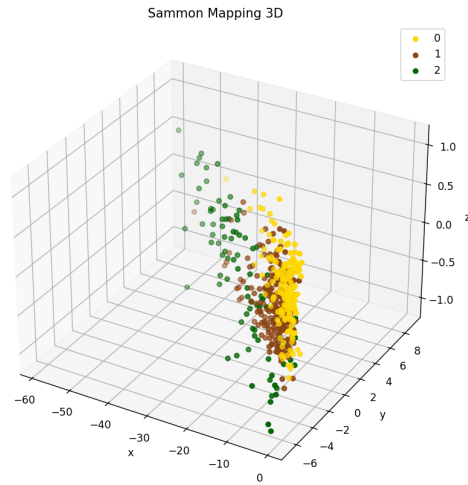


**Figure 4.1:** Gait feature projection

The plot offers a visual representation of the 3D projections derived from the Sammon Mapping technique. This remapping was generated using the top 11 most important features, as identified by the optimized Random Forest Classifier. The visualization distinctly illustrates a clear separation between the three distinct clusters. This separation highlights the efficacy of the methodology employed in capturing and distinguishing the underlying patterns within the dataset. The ability to visually discern these clusters affirms the robustness of our feature selection and classification process.

### 4.1.2 Classification

After selecting the features, a Random Forest Regressor with Leave-one-Out cross-validation was applied to the dataset, utilizing only these selected features.

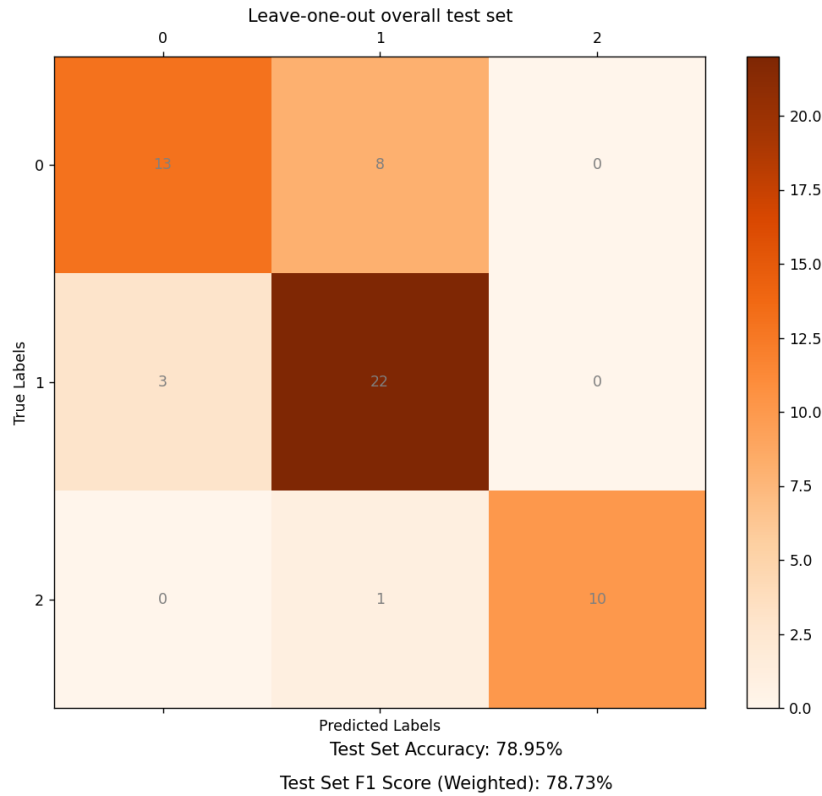


**Figure 4.2:** Gait task prediction of the score

Examining the performance of the classifier, which achieved an F1 score of 78%, reveals that the prediction accuracy is quite satisfactory. Notably, the classification of the most severe class is nearly perfect, with only one instance misclassified in the first class. This high accuracy in identifying the most severe cases is particularly commendable and demonstrates the classifier’s effectiveness in distinguishing between varying levels of severity.

### 4.1.3 Feature assessment

This section will present the distribution of the two most important features across the three classes. Additionally, it will assess these features in two example patients over several months to evaluate disease progression from the baseline to the follow-up.

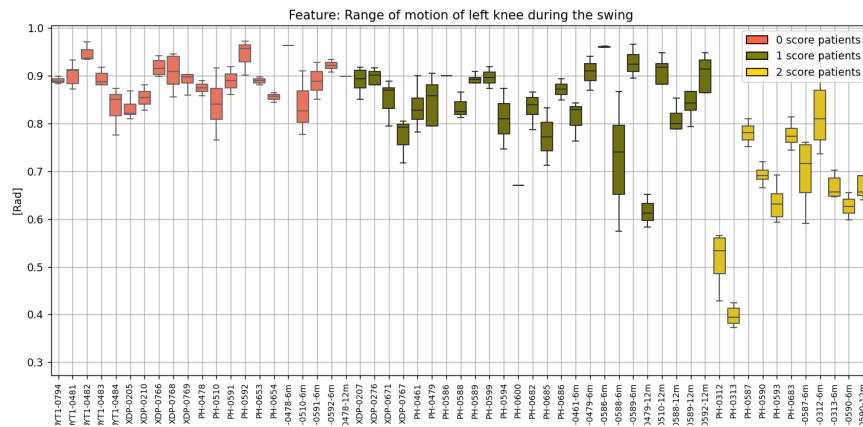


Figure 4.3: Range of motion of the left knee during the swing phase

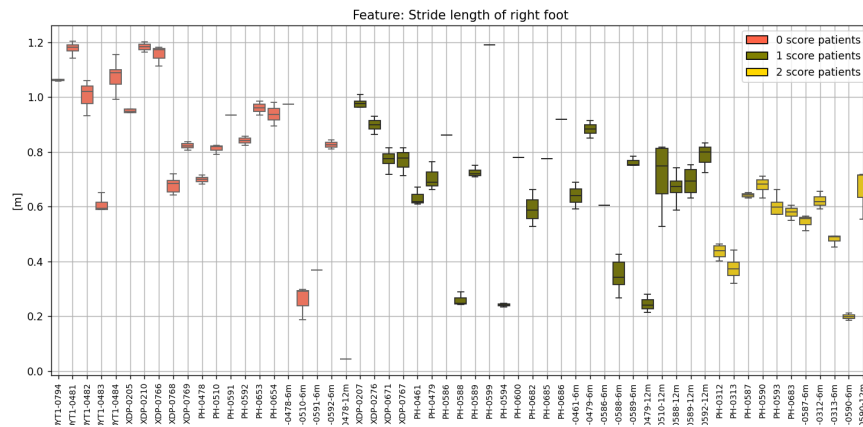
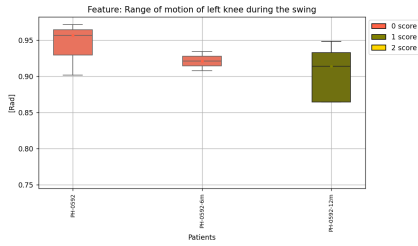


Figure 4.4: Stride length of left foot

From these two figure (figure 4.5, figure 4.4), we can observe a clear clustering among the three classes, particularly for the 'range of motion of the left knee during the swing phase' feature, which was identified as the most important by the algorithm.

## 4.1. GAIT TASK



**Figure 4.5:** Patient PH-0592: ROM left knee

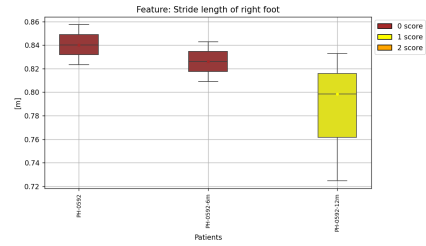


**Figure 4.6:** Patient PH-0592: stride length



**Figure 4.7:** Patient PH-0510: ROM left knee

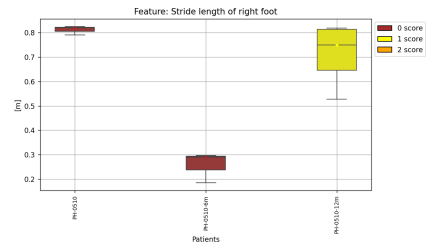


**Figure 4.8:** Patient PH-0510: stride length

The observation of feature progression in patients is one of the most significant findings from our study.

Particularly for patient PH-0592, we can observe a significant escalation in feature values from the baseline to the follow-up, which corresponds with the increasing severity of the disease. Specifically, for both features (figure 4.5, figure 4.6), there is an inverse proportionality between the disease severity and the feature values: a conspicuous progressive decrease in feature values is evident as the disease severity gradually increases.

For the second patient, PH-0510, we observe a similar trend in the first feature (figure 4.7), where the feature value changes with the severity of the disease. However, the pattern is opposite compared to the first patient: while the first patient shows a gradual decrease in feature value, the second patient exhibits a gradual increase. This difference is attributed to the distinct phenotypes of the disease observed in this study. Additionally, the second feature (figure 4.8) does not exhibit a clear trend in relation to the progression of the disease. This can be attributed to the fact that the final assessment is typically based on a combination of several features rather than relying on a single feature.

## 4.2 Freezing of gait task

For the freezing of gait task, features were evaluated on specific gait events, as previously done for the gait task. The original gait features dataset was retained, and additional specific features for this task were included, particularly focusing on the turn segments performed by patients. This focus was due to clinical insights indicating that freezing episodes primarily occur during turns.

The steps for this task remained consistent: features providing similar information were eliminated by calculating the correlation matrix, reducing the initial set from 123 features to a subset of 84 features. Subsequently, a feature selection algorithm was applied to further remove redundant information, ultimately resulting in the selection of just 7 key features.

### 4.2.1 Feature projection

This remapping (figure 4.9) was generated using the top 7 most important features, as identified by the optimized Random Forest Classifier.

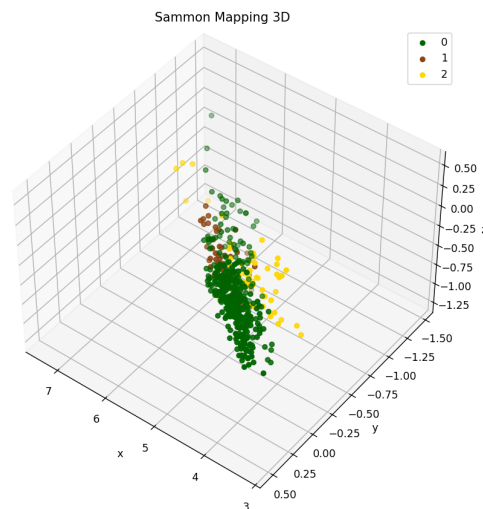


**Figure 4.9:** Freezing of gait feature projection

We can observe a reasonably good clustering among the three classes. However, the primary challenge here is the imbalance in the dataset. This imbalance may affect the classifier’s performance and the clarity

of the clustering, highlighting the need for further adjustments or techniques to address this issue.

### 4.2.2 Classification

After feature selection, a Random Forest Regressor with Leave-One-Out cross-validation was applied to the dataset.

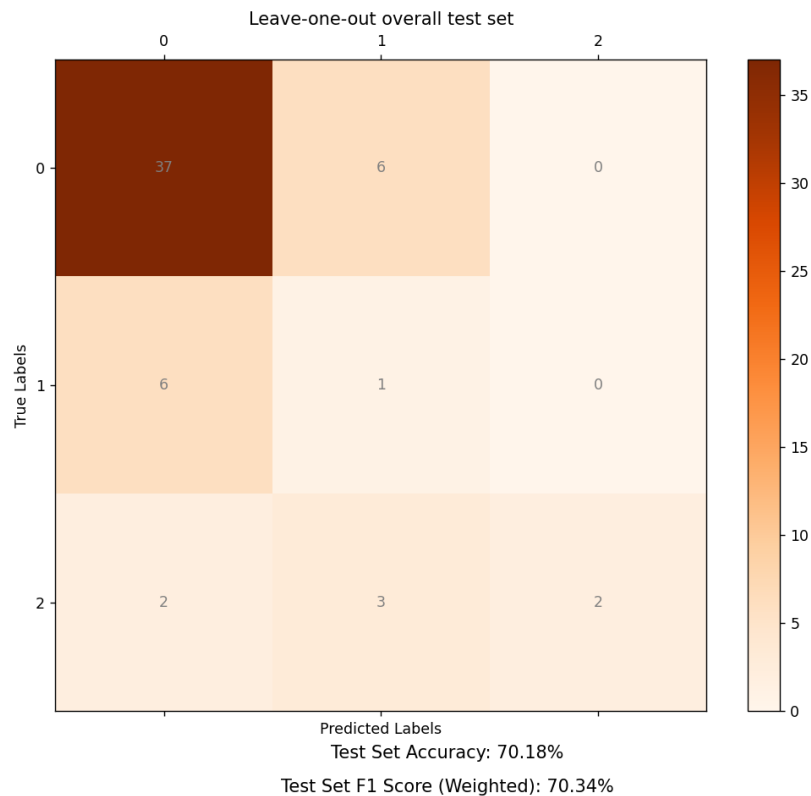


**Figure 4.10:** Freezing of gait prediction of the score

Examining the performance of the classifier (figure 4.10), which achieved an F1 score of 70%, reveals that the prediction accuracy is quite satisfactory. However, even though the classifier's performance is not particularly low, the main issue for this task, and the subsequent one analyzed in the next section, is the unbalanced dataset. The distribution of patients among the three classes is as follows:

- a. **Class 0:** 43 subjects
- b. **Class 1:** 7 subjects
- c. **Class 2:** 7 subjects

This imbalance compromises the reliability of the task evaluation, not due to the classifier setup but because of the poor distribution of subjects. Increasing the dataset size to achieve a more balanced distribution could significantly improve the task evaluation.

### 4.2.3 Feature assessment

This section will show the distribution of the two most important features across the three classes. Additionally, it will assess these features in two example patients over several months to evaluate disease progression from baseline to the 6-month follow-up.

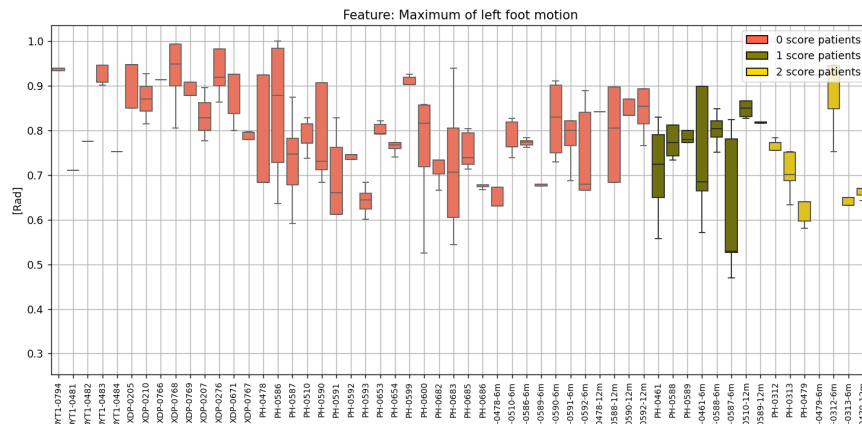


Figure 4.11: Maximum of left foot

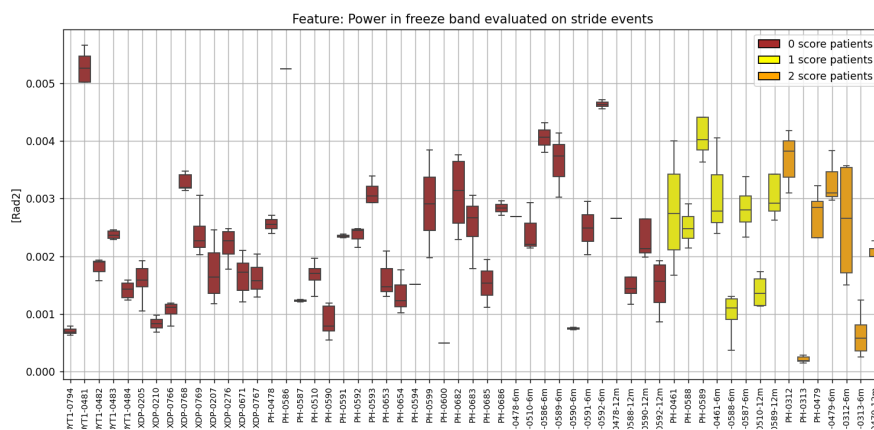
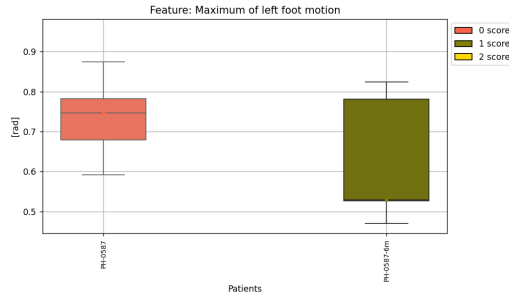


Figure 4.12: Power in the freeze band during stride events

From these two figures (figure 4.11 and figure 4.12), we can observe a wide spread in feature values among patients. There is no clear

clustering in the box plots based on the current sample size. This lack of distinct clustering suggests that the distribution could be improved with a larger dataset. Consequently, we cannot conclude that the feature is unreliable for discriminating this disease solely due to the current data limitations, particularly for the second feature.



**Figure 4.13:** Patient 0590: Maximum of left foot

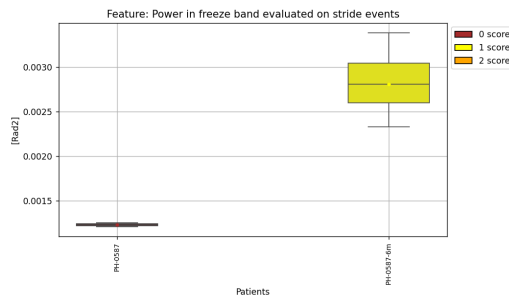


**Figure 4.14:** Patient PH-0590: Power in the freeze band during stride

Figures 4.13 and 4.14 illustrate the distribution of these two features for patient PH-0590. There is a notable change in feature values, particularly for the second feature. As observed in the gait task, these changes in feature values correspond with the increasing severity of the disease.

### 4.3 Postural instability task

The postural instability evaluation was conducted using the sliding windows technique for reasons outlined in the previous chapter. Windows with a size of 1 second and an overlap of 80% were applied to detect quantitative features from the signals. This approach increased the

number of samples per patient compared to the previous tasks, but the issue of an unbalanced dataset remains significant, as will be shown in the following sections.

The same pipeline steps were followed: calculating the correlation matrix resulted in the removal of 46 features, reducing the feature set from 88 to 42 features. Subsequently, through the feature selection algorithm, a subset of 4 features was selected.

### 4.3.1 Feature projection

This remapping (figure 4.15) was generated using the top 4 most important features, as identified by the optimized Random Forest Classifier.

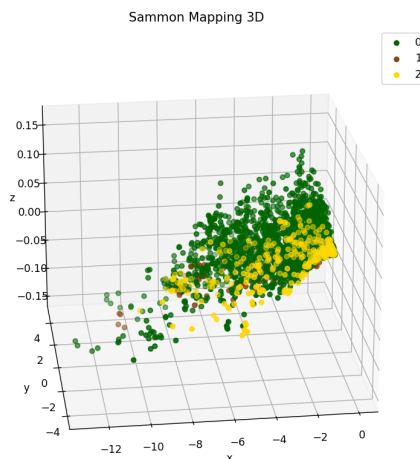


**Figure 4.15:** Postural instability feature projection

The Sammon plot shows a larger number of samples due to the application of windows for feature extraction. However, this increase in sample size is insufficient to mitigate the impact of the unbalanced dataset, resulting in suboptimal clustering between the three classes.

### 4.3.2 Classification

After feature selection, a Random Forest Regressor with Leave-One-Out cross-validation was applied to the dataset.

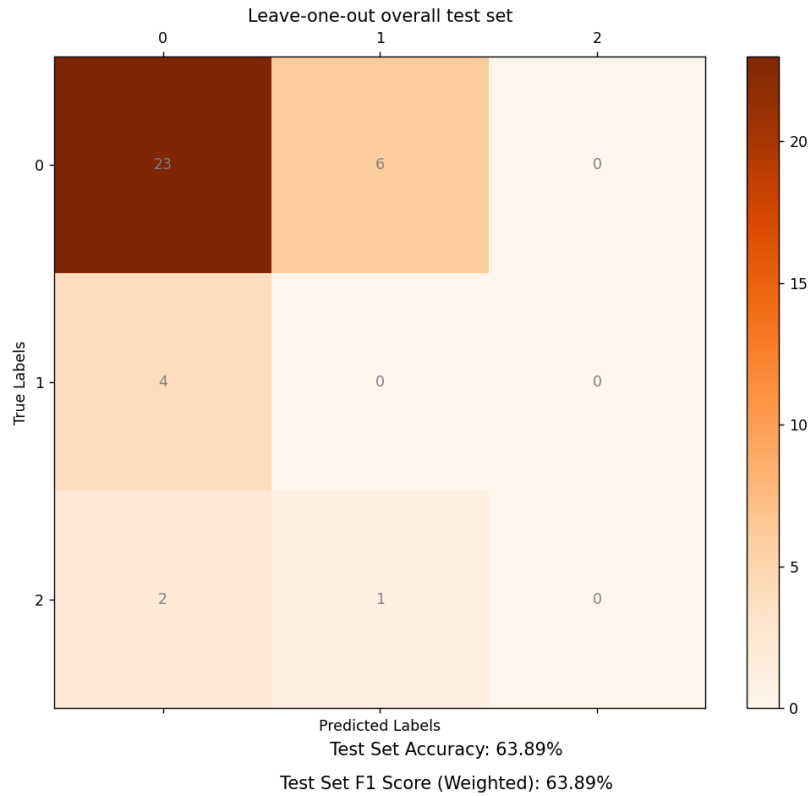


**Figure 4.16:** Postural instability classification

Analyzing the performance of the classifier (Figure 4.16), which achieved an F1 score of 63%, indicates that the prediction accuracy is inadequate. The primary issue for this task lies in the unbalanced dataset. The distribution of patients among the three classes is as follows:

- a. **Class 0:** 29 subjects
- b. **Class 1:** 4 subjects
- c. **Class 2:** 3 subjects

This imbalance significantly undermines the reliability of the task evaluation. Increasing the dataset size to achieve a more balanced distribution could substantially improve the task evaluation, especially when combined with a more precise feature evaluation.

## 5. Conclusion

The results of this study suggest that wearable technology, combined with advanced feature selection and machine learning algorithms, can be a powerful tool in monitoring and evaluating the progression of movement disorders such as XDP.

### Limitation

This preliminary exploration into the quantitative analysis of XDP also presents several limitations and aims to lay the groundwork for more in-depth future investigations.

One significant limitation of our study is the subjectivity inherent in the scoring process, which was conducted by a single clinician. This introduces potential bias, as the scores may reflect individual clinical judgment rather than a consensus view. To enhance the objectivity and reliability of assessments, future research should employ multiple clinicians or implement standardized scoring protocols.

Another major limitation is the imbalance within our dataset. The unequal distribution of samples across different labels, particularly the abundance of samples for label 0 compared to others, poses challenges for accurate analysis. This imbalance partly stems from the difficulty in data acquisition and the removal of certain subjects due to data unreliability issues, resulting in a smaller and more imbalanced dataset. Addressing this limitation would involve additional data collection efforts or applying advanced techniques, such as resampling methods, to create a more representative dataset for comprehensive analysis.

Future work should focus on refining and optimizing methodologies, exploring additional feature extraction techniques, and addressing the challenges associated with imbalanced datasets. Our findings highlight the need for a nuanced approach and pave the way for more sophisticated analyses in subsequent research endeavors.

### Conclusion

Our research contributes to the understanding and management of XDP, a complex neurological movement disorder. By focusing on the

detection of dystonic movements and utilizing the UPDRS scale for scoring, we address the critical need for more refined diagnostic tools in the clinical assessment of this disorder. The integration of sensing technology with machine learning algorithms presents a transformative approach to studying pathologies. Technologies such as IMUs, which were used in this study, provide rich streams of data capturing intricate physiological and anatomical details in real-time. Machine learning algorithms excel at extracting meaningful patterns and insights from vast datasets, enabling the identification of subtle biomarkers and disease signatures that may otherwise go unnoticed. By combining these technologies, we can gain deeper insights into the underlying mechanisms of XDP, enhance diagnostic accuracy, and personalize treatment strategies.

Our approach involves extracting features from various metrics grounded in clinical observation. This not only broadens the scope of our analysis but also ensures a comprehensive evaluation of the disorder's manifestations.

### **Future developments**

The insights from our study could be transformative for the management of this rare neurogenetic movement disorder. Providing clinicians with a more objective scoring method has the potential to significantly improve the assessment of the pathology. Additionally, applying our findings in telemedicine could benefit individuals without local support, offering a more accessible means of evaluation and support.

Further research with larger and more balanced datasets could enhance the accuracy and reliability of these methods, providing valuable insights for clinical assessments and potential use of follow-up as a test part for the classifier previously trained with the baseline dataset.

# List of Tables

3.1	Gait features table . . . . .	44
3.2	Freezing of gait features table . . . . .	45
3.3	Postural instability features table . . . . .	46

# List of Figures

3.1	IMUs sensor . . . . .	23
3.2	Accelerometer electrical circuit . . . . .	24
3.3	Gyroscope electrical circuit . . . . .	24
3.4	Magnetometer circuit . . . . .	25
3.5	Flowchart of the Kalman filter process . . . . .	26
3.6	Awinda full body strap set . . . . .	27
3.7	Full body sensor displacement . . . . .	29
3.8	Subjects involved in the study. . . . .	30
3.9	Baseline set: demographic information. . . . .	31
3.10	Follow-up set: demographic information. . . . .	32
3.11	Project pipeline . . . . .	38
3.12	Gait events detection on ankles . . . . .	40
3.13	Gait events detection on pelvis . . . . .	41
3.14	Gait events detection match . . . . .	41
3.15	Gait parameters . . . . .	42
3.16	Spatio-temporal parameters . . . . .	43
3.17	Feature selection pipeline . . . . .	47
4.1	Gait feature projection . . . . .	57
4.2	Gait task prediction of the score . . . . .	58
4.3	Range of motion of the left knee during the swing phase	59
4.4	Stride length of left foot . . . . .	59
4.5	Patient PH-0592: ROM left knee . . . . .	60
4.6	Patient PH-0592: stride length . . . . .	60
4.7	Patient PH-0510: ROM left knee . . . . .	60
4.8	Patient PH-0510: stride length . . . . .	60
4.9	Freezing of gait feature projection . . . . .	61
4.10	Freezing of gait prediction of the score . . . . .	62
4.11	Maximum of left foot . . . . .	63
4.12	Power in the freeze band during stride events . . . . .	63
4.13	Patient 0590: Maximum of left foot . . . . .	64
4.14	Patient PH-0590: Power in the freeze band during stride	64
4.15	Postural instability feature projection . . . . .	65
4.16	Postural instability classification . . . . .	66



# Bibliography

- [1] Lillian V. Lee et al. «The natural history of sex-linked recessive dystonia parkinsonism of Panay, Philippines (XDP)». In: *Parkinsonism & Related Disorders* 9.1 (2002). 6th International Symposium on the Treatment of Parkinsonism and Related Disorders, pp. 29–38. ISSN: 1353-8020. DOI: 10.1016/S1353-8020(02)00042-1. URL: <https://www.sciencedirect.com/science/article/pii/S1353802002000421> (cit. on p. 10).
- [2] D. Bragg et al. «Disease onset in X-linked dystonia-parkinsonism correlates with expansion of a hexameric repeat within an SVA retrotransposon in TAF1». In: *Proceedings of the National Academy of Sciences* 114.51 (Dec. 2017), E11020–E11028. DOI: 10.1073/pnas.1712526114 (cit. on p. 10).
- [3] LV Kalia and AE Lang. «Parkinson’s disease». In: *The Lancet* 386.9996 (Aug. 2015), pp. 896–912. DOI: 10.1016/S0140-6736(14)61393-3. URL: <https://pubmed.ncbi.nlm.nih.gov/25904081/> (cit. on p. 11).
- [4] E. Tolosa, A. Garrido, SW Scholz, and W. Poewe. «Challenges in the diagnosis of Parkinson’s disease». In: *The Lancet Neurology* 20.6 (May 2021), pp. 385–397. DOI: 10.1016/S1474-4422(21)00030-2. URL: <https://pubmed.ncbi.nlm.nih.gov/33894193/> (cit. on p. 11).
- [5] MT Hayes. «Parkinson’s disease and parkinsonism». In: *The New England Journal of Medicine* 381.10 (July 2019), pp. 932–943. DOI: 10.1056/NEJMra1716015. URL: <https://pubmed.ncbi.nlm.nih.gov/30890425/> (cit. on p. 11).
- [6] K. Grütz and C. Klein. «Dystonia updates: Definition, nomenclature, clinical classification, and etiology». In: *Journal of Clinical Medicine* 10.4 (Apr. 2021), p. 791. DOI: 10.3390/jcm10040791. URL: <https://pubmed.ncbi.nlm.nih.gov/33604773/> (cit. on pp. 12, 13).
- [7] A. Albanese, K. Bhatia, S.B. Bressman, M.R. DeLong, S. Fahn, V.S. Fung, et al. «Phenomenology and classification of dystonia: a consensus update». In: *Movement Disorders* 28.7 (2013), pp. 863–873. URL: <https://doi.org/10.1002/mds.25475> (cit. on pp. 13, 19).

- [8] M. Hallett. «Neurophysiology of dystonia: The role of inhibition». In: *Neurobiology of Disease* 42.2 (2011), pp. 177–184. URL: <https://doi.org/10.1016/j.nbd.2010.08.025> (cit. on p. 19).
- [9] V.K. Neychev, R.E. Gross, S. Lehericy, E.J. Hess, and H.A. Jinnah. «The functional neuroanatomy of dystonia». In: *Neurobiology of Disease* 42.2 (2011), pp. 185–201. URL: <https://doi.org/10.1016/j.nbd.2011.01.026> (cit. on p. 19).
- [10] S. Patel, K. Lorincz, R. Hughes, N. Huggins, J. Growdon, D. Standaert, et al. «Monitoring motor fluctuations in patients with Parkinson’s disease using wearable sensors». In: *IEEE Transactions on Information Technology in Biomedicine* 16.6 (2012), pp. 864–873. URL: <https://doi.org/10.1109/TITB.2012.2201956> (cit. on p. 19).
- [11] V.V. Shah, J. McNames, M. Mancini, P. Carlson-Kuhta, J.G. Nutt, and F.B. Horak. «Quantity and quality of gait and turning in people with multiple sclerosis, Parkinson’s disease and matched controls during daily living». In: *Journal of Neurology, Neurosurgery & Psychiatry* 91.6 (2020), pp. 590–597. URL: <https://doi.org/10.1136/jnnp-2019-322713> (cit. on p. 19).
- [12] R.S. Calabrò, G. Sorrentino, A. Cassio, M. Mazzonetto, E. Andrenelli, D.M. Bonifati, et al. «Robotic-assisted gait training in Parkinson’s disease: a three-month follow-up randomized clinical trial». In: *International Journal of Neuroscience* 128.7 (2018), pp. 688–696. URL: <https://doi.org/10.1080/00207454.2017.1417375> (cit. on p. 19).
- [13] R. Morris, S. Stuart, G. McBarron, P.C. Fino, M. Mancini, and C. Curtze. «Validity of mobility lab (version 2) for gait assessment in young adults, older adults and Parkinson’s disease». In: *Physiological Measurement* 40.9 (2019), p. 095003. URL: <https://doi.org/10.1088/1361-6579/ab3a27> (cit. on p. 19).
- [14] L. Sigcha, N. Costa, I. Pavón, S. Costa, P. Arezes, J.M. López, and J.A. Gámez. «Deep learning approaches for detecting freezing of gait in Parkinson’s disease patients through on-body acceleration sensors». In: *Sensors* 20.7 (2020), p. 1895. URL: <https://doi.org/10.3390/s20071895> (cit. on p. 19).

- [15] J. Barbič, D. Novak, and J. Podobnik. «Recognition of gait-related lower body motion using machine learning methods». In: *Biocybernetics and Biomedical Engineering* 36.2 (2016), pp. 351–362. URL: <https://doi.org/10.1016/j.bbe.2016.01.006> (cit. on p. 20).
- [16] S.T. Moore, D.A. Yungker, T.R. Morris, V. Dilda, H.G. MacDougall, and J.M. Shine. «Autonomous identification of freezing of gait in Parkinson’s disease from lower-body segmental accelerometry». In: *Journal of NeuroEngineering and Rehabilitation* 10.1 (2013), p. 19. URL: <https://doi.org/10.1186/1743-0003-10-19> (cit. on p. 20).
- [17] Daniel Rodriguez-Martin, Albert Sama, Carlos Perez-Lopez, Andreu Català, Joan Cabestany, and Alejandro Rodríguez-Moliner. «SVM-based posture identification with a single waist-located triaxial accelerometer». In: *Expert Systems with Applications* 76 (2017), pp. 158–167 (cit. on p. 20).
- [18] Martina Mancini and Fay B Horak. «Potential of APDM mobility lab for the monitoring of the progression of Parkinson’s disease». In: *Expert Review of Neurotherapeutics* 18.8 (2018), pp. 655–667 (cit. on p. 20).
- [19] Fay B Horak and Martina Mancini. «Objective biomarkers of balance and gait for Parkinson’s disease using body-worn sensors». In: *Movement Disorders* 24.S2 (2009), S32–S39 (cit. on p. 20).
- [20] Alexander Ruhe, René Fejer, and Bruce Walker. «The test–retest reliability of centre of pressure measures in bipedal static task conditions—A systematic review of the literature». In: *Gait & Posture* 32.4 (2010), pp. 436–445 (cit. on p. 20).
- [21] Martina Mancini and Fay B Horak. «The relevance of clinical balance assessment tools to differentiate balance deficits». In: *European Journal of Physical and Rehabilitation Medicine* 48.2 (2012), pp. 239–248 (cit. on p. 20).
- [22] Alan Godfrey, Rionach Conway, David Meagher, and Gearóid O’Laighin. «Direct measurement of human movement by accelerometry». In: *Medical Engineering & Physics* 30.10 (2008), pp. 1364–1386 (cit. on p. 20).

- [23] Takashi Kusaka and Takayuki Tanaka. «Stateful Rotor for Continuity of Quaternion and Fast Sensor Fusion Algorithm Using 9-Axis Sensors». In: *Sensors* 22.20 (2022), p. 7989. DOI: 10.3390/s22207989. URL: <https://doi.org/10.3390/s22207989> (cit. on pp. 23–26).
- [24] Ismael Espinoza Jaramillo, Channabasava Chola, Jin-Gyun Jeong, Ji-Heon Oh, Hwanseok Jung, Jin-Hyuk Lee, Won Hee Lee, and Tae-Seong Kim. «Human Activity Prediction Based on Forecasted IMU Activity Signals by Sequence-to-Sequence Deep Neural Networks». In: *Sensors* 23.14 (2023), p. 6491. DOI: 10.3390/s23146491. URL: <https://doi.org/10.3390/s23146491> (cit. on pp. 26, 27).
- [25] Odongo Steven Eyobu and Dong Seog Han. «Feature Representation and Data Augmentation for Human Activity Classification Based on Wearable IMU Sensor Data Using a Deep LSTM Neural Network». In: *Sensors* 18.9 (2018), p. 2892. DOI: 10.3390/s18092892. URL: <https://doi.org/10.3390/s18092892> (cit. on p. 26).
- [26] Martina Palmieri, Lucia Donno, Veronica Cimolin, and Manuela Galli. «Cervical Range of Motion Assessment through Inertial Technology: A Validity and Reliability Study». In: *Sensors* 23.13 (2023), p. 6013. DOI: 10.3390/s23136013. URL: <https://doi.org/10.3390/s23136013> (cit. on p. 27).
- [27] T. Jayalakshmi and A. Santhakumaran. «Impact of preprocessing for diagnosis of diabetes mellitus using artificial neural networks». In: (2010), pp. 109–112. DOI: 10.1109/icmlc.2010.65 (cit. on p. 38).
- [28] Martin Schepers, Matteo Giuberti, and Giovanni Bellusci. «Xsens MVN: Consistent tracking of human motion using inertial sensing». In: *Xsens Technol* 1.8 (2018), pp. 1–8. DOI: 10.1016/S1353-8020(02)00042-1. URL: <https://www.sciencedirect.com/science/article/pii/S1353802002000421> (cit. on p. 39).
- [29] DataCamp. *What is Normalization in Machine Learning? A Comprehensive Guide to Data Rescaling*. 2021. URL: <https://www.datacamp.com> (cit. on p. 39).
- [30] Bashar Alhajahmad and Musa Ataş. «Enhancing Prediction Accuracy through Normalization Techniques: Practical Insights from MLP Neural Network». In: *AS-Proceedings* 1.1 (2023), pp. 290–

295. DOI: 10.59287/as-proceedings.75. URL: <https://doi.org/10.59287/as-proceedings.75> (cit. on p. 39).
- [31] Nazir Tahira et al. «A framework for feature extraction from hospital medical data with applications in risk prediction». In: *BMC Bioinformatics* 21 (2021), pp. 1–12. DOI: 10.1186/s12859-020-03745-0. URL: <https://bmcbioinformatics.biomedcentral.com/articles/10.1186/s12859-020-03745-0> (cit. on p. 43).
- [32] Jeffrey M Hausdorff. «Gait dynamics in Parkinson’s disease: common and distinct behavior among stride length, gait variability, and fractal-like scaling». In: *Chaos: An Interdisciplinary Journal of Nonlinear Science* 19.2 (2009), p. 026113. DOI: 10.1063/1.3147408 (cit. on p. 44).
- [33] Galit Yogev, Nir Giladi, Chava Peretz, Shmuel Springer, Ely S Simon, and Jeffrey M Hausdorff. «Dual tasking, gait rhythmicity, and Parkinson’s disease: Which aspects of gait are attention demanding?» In: *European Journal of Neuroscience* 22.5 (2005), pp. 1248–1256. DOI: 10.1111/j.1460-9568.2005.04298.x (cit. on p. 44).
- [34] Meg E Morris, Robert Ianseck, Thomas A Matyas, and Jeffery J Summers. «Stride length regulation in Parkinson’s disease: Normalization strategies and underlying mechanisms». In: *Brain* 119.2 (2005), pp. 551–568. DOI: 10.1093/brain/awf053 (cit. on p. 44).
- [35] Meir Plotnik, Nir Giladi, and Jeffrey M Hausdorff. «A new measure for quantifying the bilateral coordination of human gait: effects of aging and Parkinson’s disease». In: *Experimental Brain Research* 181.4 (2007), pp. 561–570. DOI: 10.1007/s00221-007-0955-7 (cit. on p. 44).
- [36] Galit Yogev, Meir Plotnik, Chava Peretz, Nir Giladi, and Jeffrey M Hausdorff. «Gait asymmetry in patients with Parkinson’s disease and elderly fallers: when does the bilateral coordination of gait require attention?» In: *Experimental Brain Research* 177.3 (2007), pp. 336–346. DOI: 10.1007/s00221-006-0676-3 (cit. on p. 44).
- [37] Rossitza Baltadjieva, Nir Giladi, Leor Gruendlinger, Chava Peretz, and Jeffrey M Hausdorff. «Marked alterations in the gait timing and rhythmicity of patients with de novo Parkinson’s disease». In: *European Journal of Neuroscience* 24.6 (2006), pp. 1815–1820. DOI: 10.1111/j.1460-9568.2006.05188.x (cit. on p. 44).

- [38] Jeffrey M Hausdorff, Merit E Cudkowicz, Rachel Firtion, Jeanne Y Wei, and Ary L Goldberger. «Gait variability and basal ganglia disorders: stride-to-stride variations of gait cycle timing in Parkinson’s disease and Huntington’s disease». In: *Movement Disorders* 13.3 (1998), pp. 428–437. DOI: 10.1002/mds.870130310 (cit. on p. 44).
- [39] Steven Díaz, Jeannie B Stephenson, and Miguel A Labrador. «Use of wearable sensor technology in gait, balance, and range of motion analysis». In: *Applied Sciences* 10.1 (2019), p. 234. DOI: 10.3390/app10010234 (cit. on p. 44).
- [40] Sandro Mazilu, Alberto Calatroni, Erez Gazit, Daniel Roggen, Jeffrey M Hausdorff, and Gerhard Tröster. «Feature-set-engineering for detecting freezing of gait in Parkinson’s disease using deep recurrent neural networks». In: *arXiv preprint arXiv:1602.02644* (2016) (cit. on p. 45).
- [41] Ryan P Hubble, Geraldine A Naughton, Peter A Silburn, and Michael H Cole. «Wearable sensor use for assessing standing balance and walking stability in people with Parkinson’s disease: a systematic review». In: *PloS One* 10.4 (2015), e0123705. DOI: 10.1371/journal.pone.0123705. URL: <https://doi.org/10.1371/journal.pone.0123705> (cit. on p. 46).
- [42] et al. Ho Tung. «A Review of Feature Selection Methods for Machine Learning-Based Disease Risk Prediction». In: *Frontiers in Genetics* 10 (2019), p. 1234. DOI: 10.3389/fgene.2019.01234. URL: <https://www.frontiersin.org/articles/10.3389/fgene.2019.01234/full> (cit. on p. 46).
- [43] Isabelle Guyon and André Elisseeff. «An introduction to variable and feature selection». In: *Journal of Machine Learning Research* 3 (2003), pp. 1157–1182. DOI: 10.5555/944919.944968. URL: <http://www.jmlr.org/papers/volume3/guyon03a/guyon03a.pdf> (cit. on p. 49).
- [44] Leo Breiman. «Random forests». In: *Machine learning* 45.1 (2001), pp. 5–32. DOI: 10.1023/A:1010933404324. URL: <https://doi.org/10.1023/A:1010933404324> (cit. on pp. 50, 51, 54, 55).
- [45] Trevor Hastie, Robert Tibshirani, and Jerome Friedman. *The elements of statistical learning: data mining, inference, and prediction*. Springer, 2009. DOI: 10.1007/978-0-387-84858-7. URL: <https://doi.org/10.1007/978-0-387-84858-7>

- [//link.springer.com/book/10.1007/978-0-387-84858-7](https://link.springer.com/book/10.1007/978-0-387-84858-7)  
(cit. on pp. 50, 51).
- [46] Hemant Ishwaran, Udaya B. Kogalur, Ezra Z. Gorodeski, Aaron J. Minn, and Michael S. Lauer. «High-dimensional variable selection for survival data». In: *Journal of the American Statistical Association* 105.489 (2010), pp. 205–217. DOI: 10.1198/jasa.2009.tm08622. URL: <https://doi.org/10.1198/jasa.2009.tm08622> (cit. on p. 51).
- [47] Payam Refaeilzadeh, Lei Tang, and Huan Liu. «Cross-Validation». In: *Encyclopedia of Database Systems* (2009), pp. 532–538. DOI: 10.1007/978-0-387-39940-9\_565. URL: [https://doi.org/10.1007/978-0-387-39940-9\\_565](https://doi.org/10.1007/978-0-387-39940-9_565) (cit. on p. 52).
- [48] Zi Jie Choong and Michael Lau. «A Comparative Analysis of Cross-Validation Techniques for a Smart and Lean Pick-and-Place Solution with Deep Learning». In: *Electronics* 12.11 (2023), p. 2371. DOI: 10.3390/electronics12112371. URL: <https://doi.org/10.3390/electronics12112371> (cit. on pp. 52, 53).
- [49] Thomas G. Dietterich. «Approximate statistical tests for comparing supervised classification learning algorithms». In: *Neural Computation* 10.7 (1998), pp. 1895–1923. DOI: 10.1162/089976698300017197. URL: <https://doi.org/10.1162/089976698300017197> (cit. on p. 53).
- [50] John W. Sammon. «A nonlinear mapping for data structure analysis». In: *IEEE Transactions on Computers* C-18.5 (1969), pp. 401–409. DOI: 10.1109/T-C.1969.222678. URL: <https://doi.org/10.1109/T-C.1969.222678> (cit. on pp. 53, 54).
- [51] Mikhail Belkin and Partha Niyogi. «Laplacian eigenmaps and spectral techniques for embedding and clustering». In: *Advances in Neural Information Processing Systems* 14 (2002), pp. 585–591 (cit. on pp. 53, 54).
- [52] Bernhard Schölkopf, Alexander Smola, and Klaus-Robert Müller. «Kernel principal component analysis». In: *International Conference on Artificial Neural Networks* (1997), pp. 583–588 (cit. on pp. 53, 54).

- [53] Prakash Ranganathan and Shrirang Abhyankar. «Random Forest Regressor-Based Approach for Detecting Fault Location and Duration in Power Systems». In: *Sensors* 22.2 (2022), p. 458. DOI: 10.3390/s22020458. URL: <https://doi.org/10.3390/s22020458> (cit. on p. 55).
- [54] Grzegorz Dudek. «A Comprehensive Study of Random Forest for Short-Term Load Forecasting». In: *Energies* 15.20 (2022), p. 7547. DOI: 10.3390/en15207547. URL: <https://doi.org/10.3390/en15207547> (cit. on p. 55).

